Proteomic identification and characterization of novel factors involved in peroxisomal biogenesis

Songkui Cui

Department of Basic Biology

School of Life Science

The Graduate University for Advanced Studies

Contents

Abbreviation

2,4-D	: 2,4-dichlorophenoxyacetic acid
2,4-DB	: 2,4-dichlorophenoxybutyric acid
35S	: cauliflower mosaic virus 35S RNA promoter.
BiFC	: bimolecular fluorescence complementation
CAT	: catalase
CHAPS	: 3-[(3-cholamidopropyl)dimethylammonio]-1-propanesulfonate
CHAPSO	: 3-[(3-cholamidopropyl)dimethylammonio]-2-hydroxy-1-propanesulfonate
CPN60B	: chaperonin 60 beta
DDM	: n-Dodecyl β-D- Maltopyranoside
DEG15	: DEG15 endopeptidase
DMSO	: Dimethylsulfoxide
DOC	: deoxycholic acid
DRP1A	: dynamin related protein 1A
DRP3A	: dynamin related protein 3A
GFP	: green fluorescent protein
LACS7	: long-chain acyl-CoA synthetase 7
NP-40	: nonyl phenoxypolyethoxylethanol
OTG	: n-octyl β-D-thioglucopyranoside
PBP	: PEX16 binding protein
PEX	: peroxin
PMDH2	: peroxisomal NAD-malate dehydrogenase 2
PMP	: peroxisome membrane protein
PNC1	: peroxisomal adenine nucleotide carrier 1
PTS	: peroxisome targeting signal
THI	: thiolase
TUA6	: tubulin alpha-6

General introduction

1. Peroxisomes in flowering plants

Peroxisomes are single membrane bound, dynamic and multifunctional organelles with approximately 1 μm in diameter and are found in virtually all eukaryotic cells. Peroxisomes contribute to many catabolic pathways and thus are essential for all organisms. In human, several inherited diseases are known to be caused by abnormal peroxisomal functions such as Zellweger syndrome, which is characterized as a severe neurological, hepatic and renal defects resulting in death within the first few months of years after birth (Moser et al. 1991). In plants, the physiological function of peroxisomes were mostly studied by forward genetic screening that functional disruption of peroxisomes results in embryo lethality, germination arrest and increased susceptibility in pathogen (Hayashi et al. 1998, Goto et al. 2011, Yu et al. 2011). Recent studies also reviewed the involvement of peroxisomes in cuticular wax biosynthesis through the interaction with the endoplasmic recitulum (Kamigaki et al. 2009).

Depending on developmental stages, plant peroxisomes functionally differentiate into at least three different classes: glyoxysomes, leaf peroxisomes and unspecialized peroxisomes. Glyoxysomes are present in the cells of storage organs such as endosperms and cotyledons. Triglycerides that are main storage oil in seeds are degraded to fatty acids and are subsequently broken down by peroxisomal fatty acid β-oxidation, to produce acetyl-CoA as the end product. Acetyl-CoA is further converted by glyoxylate cycle in peroxisomes into succinate that is finally metabolized to sucrose as major energy for plant development (Hayashi et al. 1998, Kamada et al. 2003).

Leaf peroxisomes are present in the cells of green tissues including green cotyledons and leaves. In contrast to glyoxysomes, a different set of enzymes is present in leaf peroxisomes mediating glycolate pathway. During photorespiration, the recycle of the phosphoglycolate back to the Calvin cycle requires the enzymatic reactions inside leaf peroxisomes through glycolate pathway (Tolbert 1982). In recent studies with microscopic observation, leaf peroxisomes are observed to frequently

interact with choloroplast under light illumination and thus are proposed to be physically associated with choloroplast for efficient uptake of metabolites (personal communication with K. Oikawa).

Unspecialized peroxisomes are present in roots, stems, flowers and siliques. Basically, they contain enzymes that are present in other types of peroxisomes, such as catalase, glycolate oxidase and those of fatty acid β-oxidation. A recent study found that they are specifically involved in polyamine catabolism in root cells (Kamada et al. 2008). However, their functions are still poorly investigated compared to glyoxysomes and leaf peroxisomes.

2. Peroxisomal protein transport

2.i. Transport of peroxisomal matrix proteins by peroxisomal receptors

Unlike chloroplast and mitochondrion proteins, all of peroxisomal proteins are encoded in the nuclear genome and translated on cytosoilc ribosomes before being imported into peroxsisomes. With few exceptions, peroxisomal matrix enzymes contain two types of peroxisomal targeting signals: either PTS1 or PTS2. PTS1 is located at the extreme C-terminus and consists of consensus tripeptide variants that are [C/A/S/P]-[K/R]-[I/L/M] (Hayashi et al. 1996). More recently, novel PTS1 sequence is identified and its residues now are expanded to [F/V/G/T/L/K/I]-[G/E/T/F/P/Q/C/Y]-F and [S/A/P/C]-[R/K/N/M/S/L/H]-[L/M/I/V/I] (Lingner et al. 2011). PTS2 is an N-terminal consensus sequence of R-[A/I/L/Q]-X5-H-[F/I/L] and is relatively less conserved compared to PTS1 (Kato et al. 1996). PTS2-containing proteins are translated as precursors in the cotysol and are cleaved off after the import into peroxisomes through the action of PTS2 processing enzyme, DEG15 (Schuhmann et al. 2008). A quarter of peroxisomal enzymes contain PTS2, including those involved in fatty acid metabolism such as 3-ketoacyl-CoA thiolase, citrate synthase, malate dehydrogenase and long chain acyl-CoA oxidase.

Studies from different organisms have revealed two cytosolic import receptors: PEX5 for PTS1 and PEX7 for PTS2 (Kragler et al. 1998, Woodward and Bartel 2005). Mammalian has two isoforms of PEX5 and both mediate PTS1-containing protein transport. Only longer version of PEX5 (PEX5L) binds to PEX7 (Braverman et al. 1998, Matsumura et al. 2000, Otera et al. 2000) and also mediates PTS2 protein transport, suggesting the convergence of PTS1- and PTS2-containing protein transport in mammalian cells.

In Arabidopsis, which has a single PEX5 instead, yeast two-hybrid and bimolecular fluorescence complementation (BiFC) assay demonstrated that PEX7 directly binds to PEX5 in the cytosol and the central region containing WD40 repeat domain of PEX7 is sufficient for the interaction (Nito et al. 2002, Singh et al. 2009). Arabidopsis *pex5* mutant lacking PEX7 binding activity is defective in PEX7-mediated PTS2-containing protein transport, demonstrating that PEX5 directs PEX7 into peroxisomes in Arabidopsis (Woodward and Bartel 2005).

In some yeast, PTS2-containing protein transport does not require PEX5 but involves not only PEX7 but also functionally redundant PTS2 auxiliary proteins such as PEX18 and PEX21 in *Saccharomyces cerevisiae* (Einwachter et al. 2001). PEX18 and PEX21 are replaced by a single PEX7 docking protein PEX20 in *Neurospora crassa* (Sichting et al., 2003), *Yarrowia lipolytica* (Einwachter et al. 2001) and *Pichia pastoris* (Leon et al., 2006). And these auxiliary proteins share a common motif with mammalian PEX5L for PEX7 interaction. The lack of these auxiliary proteins in plants and mammals therefore suggests their replacement by PEX5 in these organisms.

Caenorahabditis elegans lacks PEX7 and PTS2-containing proteins. *C. elegans* orthologues of PTS2-containing proteins lacks PTS2 signals. Instead, they contain PTS1 in their C-terminus and their transport solely depends on PEX5, suggesting that PTS2 branches are absent from nematodes (Motley et al., 2000).

Even though there is a slight variation in terms of the number and kinds of peroxisomal receptors among various organisms as described above, the transport machinery into peroxisomes seems to be conserved in a higher range (Figure 1). In

the cytoplasm, PEX5 and PEX7 with their cargo of PTS1 and PTS2-containing proteins, respectively, interact with each other. The PEX5-PEX7 complex with their cargo is recruited to peroxisomal membrane on which they bind to peroxisomal docking proteins, PEX13 and PEX14. (Hayashi et al. 2000, Nito et al. 2002). Subsequently the receptors are translocated and recycled back to the cytosol. The translocation machinery of PEX5 was widely studied compared to PEX7. The free PEX5 after cargo release, upon binding with PEX14, is ubiquitinated by E2-like peroxins PEX4 (Koller et al. 1999) and its interacting protein PEX22 (Platta et al. 2007) and E3-like RING-finger peroxins PEX2, PEX10 and PEX12 (Okumoto et al. 2000, Platta et al. 2009). In yeast and mammals, the resulting ubiquitination acts as a signal for PEX5 release from peroxisomes by AAA ATPase peroxins PEX1 and PEX6 (Faber et al. 1998) that are anchored on membrane by peroxisomal membrane protein, PEX15 in yeast and PEX26 in mammals. Recently, an Arabidopsis counterpart of yeast PEX15 and mammalian PEX26 was identified (APEM9; Goto et al. 2011), suggesting that the monoubiquination of PEX5 might also occur in the plant, even though the direct evidence is still missing. In yeast and mammals, monoubiquitination of PEX5 by the addition of a single ubiquitin can alter its localization to the cytosol for next round of use, whereas polyubiquitinated PEX5 by the attachment of polyubiquitin chains is recruited to degradation pathway by 26S proteasome (Kiel et al. 2005, Platta et al. 2007).

2.ii. Transport of peroxisomal membrane proteins

Peroxisomal membrane proteins (PMP) and their regulatory mechanisms were widely studied in yeast and mammals. According to the studies in yeast and mammals, the transport of PMPs onto peroxisomal membranes are independent of peroxisomal receptors, PEX5 and PEX7. They are targeted to peroxisomes with yet unclear pathways. In initial studies, peroxisomal membrane proteins were categorized by two types based on their route to peroxisome after synthesis: type 1 peroxisomal membrane proteins including PEX3, PEX16 and PEX19 start their life from ER,

whereas type 2 peroxisomal membrane proteins including PEX2, PEX4, PEX10, PEX12, PEX13 and PEX14 are transported directly from cytosol to peroxisomal membranes where they start to mediate import of matrix proteins (Tabak et al. 2003).

However, more recent studies in mammals showed that more membrane proteins are thought to be transported via ER to peroxiomes (van der Zand et al. 2012). Accordingly, two types of peroxisomal precompartments are formed on ER subdomain consisting of PEX2, PEX10 and PEX12 or PEX13 and PEX14. Two types of peroxisomal precomparments are then budded from ER via PEX3, PEX16 and PEX19 and subsequently fused with each other by PEX1 and PEX6. This fusion allows assembly of the full peroxisomal translocons to start the import of matrix proteins. This completes the formation of maturated peroxisomes (Figure 2). It still needs to be elucidated whether plant also shares the common feature of *de novo* synthesis of peroxisomes as in yeast and mammalian, and whether all PEX protein homologs in plant maintain conserved functions.

3. Division and proliferation of mature peroxisomes

Mature peroxisomes undergo division through elongation and fission for proliferation (Figure 2). This is mediated by another peroxisomal membrane proteins such as PEX11, dynamin-related proteins (DRPs) and FISSION1 (FIS1). *Saccharomyces cerevisiae* PEX11 was the first protein identified to be involved in peroxisomal division. Ectopic expression of *ScPEX11* causes elongation and increased number of peroxisomes, whereas the *pex11* mutant displays one or two giant peroxisomes per cell (Erdmann and Blobel 1995, Marshall et al. 1995). Arabidopsis has five homologs of PEX11 (PEX11a to e) and each of these is capable of inducing elongation and/or increased number of peroxisomes (Lingard and Trelease 2006, Nito et al. 2007). DRPs are mechano-chemical enzymes or signaling GTPases that form oligomeric rings around membranes enforcing membrane fission or fusion through GTP hydrolysis. To date, three of the 16 Arabidopsis DRPs are found to be involved in peroxisome fission. Mutant of *drp3a*, *drp3b* or *drp5B* exhibits

the elongated peroxisomes in all plant tissues and reduced growth rate, suggesting that they are not only involved in the division of peroxisomes but also required for plant development which requires the cooperation of various organelles (Mano et al. 2004, Zhang and Hu 2009 and 2010). FISSION1 is proposed to be exclusively recruited to the division site to participate in final step of division after elongation (Zhang and Hu 2009).

4. Aim of this study

Even though there are increasing evidences that the plants have several unique features of peroxisomal biogenesis pathway, either the transport machinery of receptors during peroxisomal translocation or the machinery regulating peroxisomal membrane morphology and formation by peroxisomal membranes has been poorly studies in plants. The difficulty of this investigation has been attributed to the lethal phenotype of various plant mutants that have defect in a *PEX* gene. In addition, most of the *PEX* genes are expressed at low abundance so that the purification of PEX proteins with their interacting partners, which may be functionally similar or associated and therefore is an alternative way to understand the function of PEX proteins, became difficult.

The aim of this work is to elucidate the molecular mechanism of peroxisomal biogenesis including peroxisomal protein transport and membrane dynamics. To unveil the mechanism, I performed proteomic approaches to identify the protein complexes that are required during peroxisomal protein transport and that are involved in peroxisomal membrane regulation. Experimentally, PTS2 protein receptor PEX7 and peroxisomal integral membrane protein PEX16 were used as marker proteins regulating peroxisomal protein transport and membrane dynamics, respectively. Each protein was fused to GFP and overexpressed in Arabidopsis for the purpose of isolating complexes that bind with GFP fusion proteins. The use of overexpressed GFP-fusion proteins in Arabidopsis tackled the hurdles described above by allowing the efficient isolation of the complexes. Moreover, the analysis of

functions of each constituent of the complexes may provide the deep insight into the mechanism regulating PEX7 translocation into and out of peroxisomes and also the mechanism controlling peroxisomal membrane dynamics in association with PEX16.

Chapter 1

Proteomic identification of novel factors involved in peroxisomal biogenesis

1.1 Introduction

Peroxisomal biogenesis involves peroxisomal membrane formation and subsequent peroxisomal matrix protein transport. PEX16 is an essential peroxisomal membrane protein that is required for peroxisomal membrane targeting to peroxisomes to initiate the de novo synthesis of peroxisomes. In yeast, PEX16 is also involved in the regulation of peroxisomal structure since the overproduction of PEX16 in *Y. lipolytica* caused peroxisomal enlargement (Eitzen et al. 1997). The localization of PEX16 has been shown in Arabidospsis cultured cells and tobacco BY-2 suspension cells that it traffics through ER to finally peroxisomes (Karnik and Trelease. 2007). It remains unclear, however, how PEX16 regulate the initiation of peroxisomal membrane formation from ER as well as the morphology of mature peroxisomes.

PEX7 is a soluble import receptor that recognizes peroxisomal targeting signal type 2 (PTS2)-containing proteins in the cytosol and transports them into peroxisomes across peroxisomal membranes. Arabidopsis mutant having lower PEX7 level shows reduced efficiency of PTS2 protein transport and exhibits the germination defect causing its requirement of sucrose for germination (Hayashi et al. 2005, Woodward and Bartel 2005). However, the mechanism how PEX7 translocate into and out of peroxisomes, especially the later one, is still poorly understood.

Here in chapter 1, I describe the proteomic approach for the identification of novel binding proteins of PEX7 and PEX16 using Arabidospsis transgenic plants to understand the molecular machinery controlling peroxisomal matrix protein transport by PEX7 and that regulating peroxisomal formation and structure by PEX16. In addition, the proteins that were identified to make complex with PEX7 or PEX16 in this experiment after LC MS/MS analysis will be listed and discussed.

1.2 Materials and methods

Plant materials

Arabidopsis thaliana ecotype Columbia was used as wild-type plants, from which GFP-PEX7, GFP-PEX16 and GFP-PTS1 transgenic plants were derived (Mano et al., 2002, Singh et al. 2009).

Plant growth conditions

For germination, all seeds were surface sterilized in 1.7% NaClO and 0.017% Triton X-100 for 5 min and germinated in half-strength Murashige and Skoog (1/2 MS) medium containing 0.8% (w/v) agar, 100 μg ml^{-1} myo-inositol, 1 μg ml^{-1} thiamine-HCl, 0.5 μg ml^{-1} pyridoxine, 0.5 μg ml^{-1} nicotinic acid, 0.5 μg ml^{-1} 2-(*N*-morpholine)-ethanesulphonic acid (MES)-KOH (pH 5.7) and 2% (w/v) sucrose. After a cold treatment of 24 h at 4°C in the dark, plates were transferred to 22°C under continuous light to induce germination. Seedlings were then germinated at 22°C under dark condition. To grow on soil, seedlings grown on the plates for 10 d at 22°C under continuous light were transferred to soil under long-day conditions (16 h light/8 h dark) at 22°C.

Confocal laser scanning microscopic observation

For imaging, sample was mounted in Mili-Q (Millipore) water and imaged with a Zeiss LSM 510 confocal laser-scanning microscope. 488-nm laser was used for excitation of GFP. For emission, 505- to 530-nm band pass filters was used.

Immunoblot analysis

Total proteins were extracted from each plant by homogenization with sample buffer [10 mM Tris-HCl pH 6.5, 12% (v/v) glycerol, 5% (v/v) 2-mercaptoethanol and 1% (w/v) sodium dodecyl sulfate]. Protein concentration was measured using Bio-Rad protein assay (Bio-Rad Laboratories) with bovine gamma albumin as the standard. Equal amounts of proteins, as well as a standard molecular

marker (Pre-stained Low Range, Bio-Rad), were separated by SDS-PAGE and transferred to a Millipore GVHP (0.22μm) membrane. Membranes were blocked in 5% (w/v) skim milk solubilized in TBS-Tween [50 mM Tris-HCl, 0.15 M NaCl, 0.05% (w/v) Tween-20, pH 7.5] for 1 h with shaking, immunolabeled with primary (1.5: 10,000 v/v) and secondary (5:10,000 v/v, ECL Anti-Rabbit IgG, GE Healthcare) antibodies, and visualized with Chemi-Lumi One reagent (Nacalai Tesque).

Protein solubilization

Seedlings overexpressing GFP-PEX16 were homogenized using sampling buffer containing Triton X-100, Tween 20, OTG, SDC, CHAPS, CHAPSO, NP-40, DDM, digitonin or SDS with indicated concentration in the Figure 1.4. Total homogenates were partially applied to ultracentrifugation at 100,000 × *g* for 20 min to separate into cytosol and membrane fractions. Equal amount of proteins from each fraction were applied for immunoblot analysis whose procedure was described above.

Immunoprecipitation

Immunoprecipitation experiment was performed using μMACS Epitope Tag Protein Isolation Kits (Miltenyi Biotec). The whole seedlings of transgenic plants overexpressing GFP-PEX7, GFP-PTS1 or GFP-PEX16, which were grown under dark condition, were homogenized with homogenization buffer containing 50 mM HEPES-NaOH, pH8.0, 150 mM NaCl and 0.25% (w/v) digitonin or 0.1% (w/v) n-dodecyl β-D- maltoside (DDM) on ice. The homogenates were subjected to centrifugation at 100,000 × *g* for 30 min at 4˚C. The collected supernatants were incubated with magnetic beads conjugated to an anti-GFP antibody (Miltenyi Biotec) for 30 min on ice. The mixtures were then applied to μ Columns (Miltenyi Biotec) which were attached to magnetic field to capture the magnetic antigen-antibody complexes. The columns were washed by homogenization buffer for several times, followed by addition of elution buffer (Miltenyi Biotec) to elute the immunoaffinity complexes.

Peptide preparation for MASS spectrometry analysis

To digest the isolated protein complexes into peptides, we applied in gel digestion. The elute fractions were subjected to SDS-PAGE, and the gel was collected and washed twice by distilled water (for LC/MS; KANTO CHEMICAL CO., INC.), three times by 30% (v/v) acetonitrile for 1 h, once by 100% acetonitrile for 10 minutes and then dried by vacuum. The dried gel was deoxidized by deoxidization buffer containing 10 mM dithiothreitol and 25 mM ammonium bicarbonate for 1 h at 56 ˚C, alkylated by alkylation buffer containing 55 mM iodoacetamide and 25 mM ammonium biocarbonate for 45 min at 25 ˚C, washed twice by 25 mM ammonium bicarbonate, dehydrated twice by dehydration buffer containing 50% (v/v) acetonitrile and 25mM ammonium bicarbonate for 10 min and once by 100% (v/v) acetonitrile for 5 min, and then treated by 0.1 mg/ml trypsin (sequence grade; Promega) in 25mM ammonium bicarbonate for 16 h at 37 ˚C. The digested peptides were recovered by 5% formic acid in 50% acetonitrile and 0.1% acetic acid in 5% acetonitrile, respectively. The extracted peptides were combined and subjected to centrifugation at 13,000 × *g* for 3 min using 0.45 μm filter (MILLIPORE, Ultra free-MC 0.45 μm Filter Unit) to remove any debris. The samples were then subjected to mass-spectrometric analysis using an LTQ-Orbitrap (Tamura et al. 2010).

1.3 Results

Establishment of transgenic plants

In our initial attempts to isolate binding proteins of PEX7 or PEX16, we constructed a chimeric gene encoding GFP fused to Arabidopsis PEX7 or PEX16 under control of the cauliflower mosaic virus 35S promoter (Figure 1.1A). In parallel, a construct encoding GFP fused PTS1 consists of three amino acids (SKL) was prepared. As GFP-PTS1 targets into peroxisomes, we prepared it as a negative control for the following experiments. Each construct was inserted into Ti vector and then transformed into wild-type Arabidopsis (ecotype Columbia) using *Agrobacterium tumefaciens*. In this way, transgenic Arabidopsis progenies overexpressing GFP-PTS1, GFP-PEX7 or GFP-PEX16 were selected (Figure 1.1B). Post-germinative growth of GFP-PTS1 and GFP-PEX16 plants were similar to wild-type plant. Even though mature GFP-PEX7 plant was slightly dwarf than wild-type plant, no pale-green leaves were observed, which is typical phenotype of leaf peroxisomal defect previously reported (Hayashi et al. 2005, Schumann et al. 2007). It suggests that overexpression of GFP-PTS1, GFP-PEX7 or GFP-PEX16 does not affect leaf peroxisomal function in *Arabidopsis*.

Subcellular localization of each fusion protein

To determine the subcellular localization of each fusion protein, confocal microscopic observation into the cells of each transgenic plant was conducted. As shown in Figure 1.1C, GFP-PTS1 was targeted to peroxisomes showing individual green punctate structures. GFP-PEX7 was observed not only in peroxisomes but also in cytosol as the green signal is widely diffused in the inter-space of each cell. GFP-PEX16 is localized on peroxisomes. When GFP-PEX16 is overexpressed, the peroxisomes turned into aggregates (Figure 1.1C) that were found to be originated from dispersed peroxisomes in the cytosol (data not shown). On average, a single aggregated particle with a diameter of 5 μm is existed in each cell, suggesting that overexpression of GFP-PEX16 protein changes the distribution of peroxisomes.

Determination of detergent for efficient solubilization of fusion proteins

Apart from GFP-PEX7 and GFP-PTS1 that are soluble proteins, GFP-PEX16 is a peroxisomal membrane protein. Solubilizing membrane proteins with their own integrity is a critical step for protein complex purification in immunoprecipitation experiment. Therefore, prior to the purification of protein complex, the condition in which GFP-PEX16 is sufficiently solubized was first tested using various detergents. High concentration of either ionic (SDC, DOC) or non-ionic (Triton X-100, Tween 20, OTG, CHAPS, CHAPSO, NP-40, digitonin, DDM) detergents were tested in the extracts of GFP-PEX16 seedlings (Figure 1.2A). One percent of SDS as a strong ionic detergent capable of solubilizing most of integral membrane proteins was used as a positive control. As a result, GFP-PEX16 was well solubilized by the treatment of DDM and digitonin as well as by SDS, which allowed me to determine the minimum concentration of these two detergents in order to maintain the integrity of GFP-PEX16 complex as much as possible. Various concentrations of DDM and digitonin were then tested. As a result, 0.1% of DDM (Figure 1.2B) and 0.25 % of digitonin (Figure 1.2C) appeared to sufficiently solubilize GFP-PEX16 as a peroxisomal membrane protein.

Isolation of protein complexes containing PEX7 or PEX16

Having established transgenic plants and lowest concentration of detergents, protein complexes of GFP-PEX7 and also GFP-PEX16 proteins were purified by immunoprecipitation using antibody against GFP. As shown in Figure 1.3, seedlings of GFP-PTS1, GFP-PEX7 and GFP-PEX16 grown for 7 days in the dark were prepared. Proteins were extracted from whole tissues using two types of homogenization buffer, one containing 0.1% DDM and the other containing 0.25% digitonin. Subsequently, these extracts were applied to immunoprecipitation using anti-GFP antibody.

All fusion proteins appeared to be sufficiently immunoprecipitated as shown from their existence in the purified fractions (Figure 1.4A). In parallel, the

purified fraction from each sample was subjected to separation by SDS-polyacrylamide gel electrophoresis followed by silver staining to visualize whole protein complexes (Figure 1.4B). In addition to the fusion protein itself in each lane, there were a number of additional proteins. Some of them were only specific in the lane of GFP-PEX7 while some were specific in GFP-PEX16. For example, in Figure 1.4B, the band pattern in GFP-PEX7 sample was very similar between digitonin and DDM experiment whereas many of them did not appear in any of GFP-PTS1 or GFP-PEX16 samples. This result indicates that two detergents are likely to solubilize the same fusion protein with similar integrity and also that fusion proteins might be isolated with their specific binding proteins.

Identification of binding proteins of PEX7 or PEX16 by MS analysis

To identify the affinity purified proteins, the purified fractions of GFP-PTS1, GFP-PEX7 and GFP-PEX16 were applied to mass spectrometry analysis using LTQ-Orbitrap after trypsin in gel digestion. To exclude proteins nonspecifically bind with the GFP-fusion proteins, we first selected proteins that simultaneously appeared both in DDM and digitonin solubilized samples from each plant type. As a result, a total of 33, 119 and 72 proteins were detected in both of DDM and digitonin treated samples of GFP-PTS1, GFP-PEX7 and GFP-PEX16, respectively (Figure 1.5A). Moreover, proteins with high MASS scores were selected exclusively by removing proteins with scores lower than 50 and subsequently compared among three plant types (Figure 1.5B). As a result, a total of 15 proteins were identified specifically in GFP-PEX7 sample (Figure 1.5B, Table 1.1), whereas they were absent in GFP-PTS1 and GFP-PEX16 samples. One of them is well known binding protein of PEX7, that is PEX5, a peroxisomal receptor of PTS1-containing proteins. Likewise, 3 and 1 proteins were exclusively identified in GFP-PEX16 (Table 1.2) and GFP-PTS1 (Table 1.3) samples, respectively. Two proteins identified in GFP-PEX16 sample are novel proteins with unknown biological functions. They were named as PEX16-binding protein 1 (PBP1) and 2 (PBP2), respectively, in this study. In addition, 6 proteins were commonly identified both in DDM and digitonin treated samples of GFP-PEX7

and GFP-PEX16 but not in GFP-PTS1 (Table 1.4). Ten proteins were identified both in DDM and digitonin treated samples of all of three different seedlings (Table 1.5). As shown in Table 1.4 and Table 1.5, almost all the proteins were transcription factors or those highly expressed in seeds locating on protein body or oil body. These are obviously not peroxisome-related and thus suggested as contaminants that were nonspecifically precipitated with fusion proteins. Only one protein was specifically identified with GFP-PTS1 whereas it encodes a protein that is located on apoplast and cell wall regulating mucilage metabolic process for seed coat development, suggesting that it is also a contaminated protein.

1.4 Discussion

Protein complex isolation by coimmunoprecipitation with improved specificity

In this study, GFP was fused to PEX7 and PEX16 and these constructs driven by 35S promoters were individually introduced into *Arabidopsis theliana* ecotype Columbia by Agrobacterium transformation. Based on the fusion proteins of GFP-PEX7 and GFP-PEX16 being highly produced, antibody against GFP could efficiently target and purify these proteins by immunoprecipitation. However, it is still difficult to remove the contaminants that are nonspecifically eluted together with the target protein of my interest.

It is difficult for immunoprecipitation experiment to remove non-specifically binding proteins during complex isolation. And it was the case for this experiment. As the MS data indicated, more than one hundred proteins were identified as GFP-PEX7 and GFP-PEX16-binding proteins (Figure 1.5A). Based on the already published data and annotation for subcellular localization, it was turned out that most of the proteins are localized on various organelles rather than peroxisomes. However, these contaminated proteins were efficiently eliminated by three criteria based on the comparison of proteins after MASS analysis. First (criteria 1), each plant sample was subjected to the same experiments by the treatment of two different detergents. Subsequently, the proteins identified in both detergents were exclusively selected as potential candidates. As a result, more than half of proteins were excluded in this way. For example in Figure 1.5A, 119 proteins were screened from more than 200 proteins that were coimmunoprecipitated with GFP-PEX7 protein. Second (criteria 2), the candidates appeared in both detergents were compared with negative controls. For example, proteins identified with GFP-PEX7 sample were compared with those with GFP-PTS1 and GFP-PEX16 samples, and then the common proteins in all of three samples were further excluded as contaminants. Finally (criteria 3), the proteins with protein score over 50 by MASS analysis were selected as highly potential candidates. The protein score is a statistical score that is calculated by Mascot search engine (Matrix Science) for how well the experimental

data matches the database sequence. Basically, the statistically high score reflects the high probability as binding proteins. Overall, a few proteins were finally confined as the candidates of binding proteins with relatively higher specificity.

The advantage of this coimmunoprecipitation experiment by comparison of proteins after MS analysis is that it significantly reduces the time in the way of determining the candidates with the first priority. Because it minimize the total number of candidates, the confirmation of the binding activity can be quickly tested by other binding assays such as bimolecular fluorescence complementation (BiFC) test and yeast two hybrid system. If no proteins were found as positive, others that were excluded by criteria 3 or criteria 1 could be tested as a second priority.

However, it should be noted that there is still a possibility of specific binding proteins being eliminated in these criteria applied. As table 1.6 indicated, 2 PTS2-containing proteins which are already known binding targets of PEX7, are eliminated after criteria 1 as they were identified only in one detergent (DDM) and thus were eliminated as contaminants together with 299 proteins (Figure 1.5A). It indicates that PTS2 and PEX7 complexes are relatively stable in DDM compared to that in digitonin and further suggests that the stability of proteins varies in different detergent. This result indicates that it is important to change the combination of criteria (such as criteria 2 and criteria 3 without criteria 1 or vice versa) depending on different purposes.

Peroxisomal targeting of GFP-tagged PEX7 fusion protein

In line with PEX7 function as a PTS2 receptor in cytosol and previous report of PTS2-containing protein import into peroxisomes in yeast and mammalian cells (Zhang and Lazarow1995, Braverman et al. 1998), it was observed that GFP-fused PEX7 (GFP-PEX7) protein was localized in the cytosol in Arabidopsis GFP-PEX7 transgenic plant (Figure 1.1C; Singh et al. 2009). In addition to cytosol, significant amount of GFP-PEX7 is existed in peroxisomes compared to endogenous PEX7, which is mainly in cytosol (Singh et al. 2009). The different subcelluar localization between GFP-PEX7 and endogenous PEX7 will be described and deeply

discussed in Chapter 2. In the leak epidermal cells, such dual localization of transiently expressed GFP-PEX7 was also observed as that in Arabidopsis GFP-PEX7 transgenic plant. This permissive result for the GFP-PEX7 localization indicates the similar behavior between the fusion protein and endogenous PEX7 at least on the import process in which it was described that endogenous PEX7 recognized PTS2 cargo in the cytosol followed by the peroxisomal membrane docking through interaction with one of docking complex PEX13 (Singh et al. 2009). Thus, the transgenic line of GFP-PEX7 plant is a useful tool for studying the mechanism of PEX7-mediated peroxisomal protein transport.

Novel proteins that make complexes with PEX7

A total of 14 proteins were specifically identified as highly potential binding partners of PEX7. All of them are not annotated or reported to be localized on peroxisomes except PEX5, which is a PTS1 receptor for peroxisomal import. PEX5 binds PEX7 in the cytosol in all eukaryotes (Nito et al. 2002, Matsumura et al. 2000) indicating that the coimmunoprecipitation successfully captured these two proteins.

Among them, 10 proteins are chaperonin proteins. Nine of them are the subunit of T-complex, which is a cytosolic chaperonin that is relatively well studied in animals (Lewis et al. 1992, Yaffe et al. 1992, Kubota et al. 1994). This complex consists of two identical stacked rings, each containing eight different proteins. Arabidopsis genome contains 9 genes: T-complex subunit α, β, γ, δ, ε, ζ1, ζ2, η and θ, which are similar to those of mouse Tcp-1 (T-complex). It should be noted that all of these subunits were identified in this study, suggesting that T-complex may bind PEX7 in the cytosol in Arabidopsis. T-DNA insertion lines are absent in seed stock center except ζ1 and ζ2. The Arabidopsis mutant of ζ1 and ζ2 subunits were examined previously and turned out to be normal in terms of plant growth and peroxisomal function. The double mutant of ζ1 and ζ2 were appeared lethal in embryo (data not shown). Therefore, T-complex seems to be essential for plant but the function is still not known. Previous studies using affinity purification revealed that T-complex binds many of its substrates containing WD40 repeat domain in yeast and mammals

(Valpuesta et al. 2002, Yi et al. 2006). As PEX7 is largely composed of WD-40 domain, it is tempting to speculate that PEX7 and its cargos as well as PEX5 may be stabilized by T-complex through the direct binding. In addition, CHAPERONIN 60 β (CPN60B) was found as another chaperonin with GFP-PEX7. T-complex and CPN60 together with HSP60 chaperone are categorized in the same family suggesting that both proteins may share similar function or contribute differently on PEX7 translocation.

DYNAMIN RELATED PROTEIN 1A (DRP1A) was already characterized and localized in cell plate during cell division (Fujimoto et al. 2008), based on the microscopic observation of GFP fusion proteins. As PEX7 is both cysotolic and peroxisomal, this protein is less likely to bind PEX7 indicating that it is probably unspecific binding protein that was coimmunoprecipitated with GFP-PEX7.

In addition, two small GTPases family proteins, RabE1c and RabA1e, were identified. Interestingly, the closest homologs of mammalian RabE1c, named Rab8a, was found in peroxisomes (Hotchin et al. 2010). Therefore, both RabE1c and RabA1c were fused with GFP and expressed transiently in leak epidermal cells (see Chapter 2). Only RabE1c was localized in peroxisomes, whereas RabA1e was not. The interaction between RabE1c and PEX7 was further analyzed by BiFC. As a result, they interacted with each other in vivo. This result indeed indicates that RabE1c is a novel binding partner of PEX7 which is identified in this proteomic identification.

Novel binding proteins for PEX16

To date, there are no proteins reported to bind PEX16. In this proteomic study, two proteins were specifically identified as binding proteins of PEX16. According to TAIR database, they are 'MYOSIN HEAVY CHAIN-RELATED DOMAIN' (named PBP1) and 'ARM REPEAT SUPERFAMILY PROTEIN' (named PBP2) with unknown function. On the other hand, the proteins excluded as contaminants in GFP-PEX16 protein were clearly turned out to be contaminations based on the published data and annotated localization.

Myosins are categorized as large superfamily of molecular motors, which generate molecular forces in interaction with actin filaments. Peroxisomes move in acto-myosin dependent manner (Jedd and Chua 2002). Since there is a lack of information about the domain in PBP1, a question remained whether this protein is truly a motor protein. Based on this question, it raises a speculation that PBP1 is involved in the movement or the positioning of peroxisomes through PEX16 binding, because it was shown in the previous report that PEX16 is also involved in the spatial distribution of peroxisomes by accelerating aggregation of peroxisomes (Lin et al. 2004).

PBP2 protein possesses a domain with an armadillo (ARM)-like fold, consisting of a multi-helical fold comprised of two curved layers of alpha helices arranged in a regular right-handed superhelix. This superhelical structure has a capacity of binding large substrates and found in a number of proteins with various functions, including importins, exportins, protein kinase and RNA-binding proteins. The function of PBP2 on PEX16 with its relation to peroxisomal biogenesis should be determined by the mutant analysis.

Chapter 2

Functional characterization of RabE1c as a binding partner of PEX7

2.1 Introduction

In Arabidopsis, there are 220 putative PTS1-containing proteins and 60 putative PTS2-containing proteins. They are imported into peroxisomes by two soluble receptors, PEX5 and PEX7, respectively (Kragler et al. 1998, Woodward and Bartel 2005). The binding of PEX7 to PEX5 in the cytosol is a prerequisite for the import of PEX7-PTS2 cargo complex but not for PEX5-PTS1 cargo complex (Woodward and Bartel 2005), indicating the PEX5-dependent PEX7 protein import. Compare to its import pathway, the mechanism of PEX7 dislocation into the cytosol is poorly characterized.

Although PEX7 is important for peroxisomal protein transport, it is not known whether the other associate proteins, which regulate PEX7 function, exist or not. Proteomic analysis of PEX7 binding proteins using Arabidopsis transgenic plants overexpressing GFP - tagged PEX7 has identified a small GTPase RabE1c as one of the novel binding components to PEX7 as described in Chapter 1. Although several reports indicate the involvement of Rab GTPases in peroxisomal function in mammalian cells (Verheyden et al. 1992, Fransen et al. 2008, Anthonio et al. 2009, Hotchin et al. 2010), little is known about their roles on PEX7 behavior. In this study, we have conducted the biochemical experiments and mutant analysis with the aim of understanding RabE1c function on PEX7. We showed that RabE1c and PEX7 indeed interact with each other *in vivo*. In addtition, we showed that RabE1c is part of the PEX7 export machinery and is involved in PEX7 degradation.

2.2 Materials and methods

Plant materials and growth conditions

Arabidopsis thaliana (Columbia accession) wild-type, *rabe1c* mutant, *pex7i* knockdown and transgenic GFP-PTS1, GFP-PEX16, GFP-PEX7 plants were used. The detail of *pex7i* knockdown plant was described previously (Hayashi et al. 2005). The detail of GFP-PTS1, GFP-PEX16, GFP-PEX7 transgenic plants was described in Chapter 1. A *rabe1c* knockout mutant (SALK_055451) was obtained from the Arabidopsis Biological Resource Center (ABRC). The presence of a T-DNA insertion was confirmed by PCR with a RabE1c-specific primer conjugated with *attB1* at 5' end (5'-AAAAAGCAGGCTCAATGGCTGCTCCACCTGCT-3') and the T-DNA-specific primer SALK LBa1 (5'-TGGTTCACGTAGTGGGCCATCG-3'). The *rabe1c* mutant was crossed with GFP-PEX7 to generate a GFP-PEX7/*rabe1c* transgenic plant. These plants were grown on germination medium containing 0.8% (w/v) agar, half-strength Murashige-Skoog (MS) salts, 100 μg ml^{-1} myo-inositol, 1 μg ml^{-1} thiamine-HCl, 0.5 μg ml^{-1} pyridoxine, 0.5 μg ml^{-1} nicotinic acid, 0.5 μg ml^{-1} 2-(*N*-morpholine)-ethanesulphonic acid (MES)-KOH (pH 5.7) and 2% (w/v) sucrose. In some experiments, 2,4-dichlorophenoxybutyric acid (2,4-DB) was added, or sucrose was removed from the growth medium (as indicated). Germination was induced under continuous white light conditions at 22°C following incubation in the dark for 48 h at 4°C. For treatment with proteasome inhibitors, 4-day-old dark-grown seedlings were vacuum-infiltrated with liquid MS medium containing 0.5% (v/v) dimethylsulfoxide (DMSO) and 50 μM MG132 or 5 μM lactacystin for 10 min and then incubated in the dark for 3 h. Control plants were treated with liquid MS medium containing 0.5% (v/v) DMSO.

Plasmid construction

To generate the *GFP-RabE1c* and *GFP-RabA1e* constructs, cDNA fragments of each gene with *attB1* and *attB2* attached at their 5' and 3' ends, respectively, were amplified by RT-PCR using gene-specific primer sets (for *GFP-*

RabE1c, 5'-AAAAAGCAGGCTCAATGGCTGCTCCACCTGCT-3' and 5'-AGAAAGCTGGGTTTTAAGTTCCACAGCATGCAG-3'; for *GFP-RabA1e*, 5'-AAAAAGCAGGCTTAATGGGAGCCTACAGAGCC-3' and 5'-AGAAAGCTGGGTCTCAACCTGAGCAACAACCA-3') and cloned into the entry vector pDONR221 using the Gateway BP recombination method (Invitrogen). Subsequently, the vectors were transferred into the destination vector pUGW52 (kindly provided by Dr. Nakagawa, Shimane University; Nakagawa et al. 2007) using the Gateway LR recombination method (Invitrogen).

BiFC assays

The cDNAs of *RabE1c* and *PEX7* were cloned into pDONR221 and subsequently transferred into the destination vector pGWcY and pnYGW (kindly provided by T. Nakagawa; Singh et al. 2009, Hino et al. 2011), respectively, to generate *RabE1c-cYFP* and *nYFP-PEX7,* using BP and LR recombination methods described above (Invitrogen). The expression vector ptdGW (a gift from Dr. R. Y. Tsien, University of California), harboring the *tdTomato* gene was used as a marker for transformation, and the vector ptdTomato-PTS1, harboring the *td-Tomato-PTS1* gene (Singh et al., 2009), was used as a marker for peroxisomes.

Standard procedures for transient expression experiment were described previously (Singh et al., 2009). Mixtures of the appropriate combinations of plasmids were coated on gold particles 1.0 μm in diameter and bombarded into leek epidermal cells using the PDS-1000/He Biolistic Particle Delivery System (Bio-Rad), resulting in coexpression of these proteins in the same cells after 20 h incubation in the dark at room temperature. Imaging analysis of transfected cells was performed using confocal laser scanning microscopy.

Confocal laser scanning microscopy

The leek epidermis was observed with a Zeiss LSM 510 confocal laser scanning microscope. The 488, 514, and 543 nm lasers were used for excitation of

GFP, YFP, and RFP, respectively. For emission, 505-530 nm band–pass (GFP), 520-555 nm band-pass (YFP), and 560-615 nm band-pass (RFP) filters were used.

Immunoblot analysis

The preparation of samples and subsequent application to SDS-polyacrylamide gel electrophoresis, immunodetection and the concentration of antibodies were the same as those in the Materials and methods described in Chapter 1.

For subcellular fractionation, seedlings were homogenized in a high-salt buffer [150 mM HEPES-KOH (pH 7.5), 500 mM NaCl], followed by centrifugation at 100,000 × *g* for 20 min to separate the soluble and membrane fractions. Equal amounts of proteins from each fraction were subjected to immunoblot analysis.

2.3 Results

RabE1c interacts with PEX7 and partially localizes on peroxisome

Two small GTPases, RabE1c and RabA1e, were newly identified in our experiment (Table 1.1). We examined the subcellular localization of RabE1c and RabA1e by transiently expressing GFP-RabE1c and GFP-RabA1e in leek epidermal cells (Figure 2.1). GFP-RabE1c was observed predominantly in the cytosol, peroxisomes, and unidentified particles (Figure 2.1A). The punctate structures distinct from the peroxisomes might represent the Golgi complex, because RabE1d, another member of the RabE1 family, is localized to the Golgi complex and cytosol in Arabidopsis (Zheng et al. 2005). GFP-RabA1e was localized in the cytosol and to particulate structures distinct from peroxisomes (Figure 2.1B). These results suggest that RabE1c interacts with PEX7 on the peroxisome.

To confirm the interaction between PEX7 and RabE1c *in vivo*, we performed a BiFC assay. To this end, we constructed two chimeric genes, one encoding the N-terminal half of YFP fused to PEX7 (nYFP-PEX7) and other encoding the C-terminal half of YFP fused to RabE1c (RabE1c-cYFP). These proteins, along with tdTomato-PTS1, a peroxisomal marker, were transiently expressed in leek epidermal cells. As shown in Figure 2.2A, YFP fluorescence was observed exclusively on peroxisomes, as identified by the red fluorescent signal of tdTomato-PTS1. No signal was detected in control cells expressing RabE1c-cYFP and nYFP (Figure 2.2B) or cYFP and nYFP-PEX7 (Figure 2.2C). These results indicate that PEX7 and RabE1c specifically interact with each other on peroxisomes *in vivo*.

The active form of RabE1c interacts with PEX7

To determine whether GTP binding is crucial for the interaction of RabE1c with PEX7, we generated three mutant forms of RabE1c containing amino-acid substitutions: Ser29 to Asn (RabE1c[S29N]), Gln74 to Leu (RabE1c[Q74L]), and Asn128 to Ile (RabE1c[N128I]). In many Rab- and Ras-like GTPases, these amino-

acid substitutions correspond to RabE1c mutations that alter nucleotide affinity, resulting in either a GDP-bound dominant-negative form or a GTP-bound constitutively active form (Bourne et al. 1991). RabE1c[S29N] and RabE1c[N128I] are predicted to be the GDP-bound dominant-negative forms, and RabE1c[Q74L] should produce the GTP-bound constitutively active form. Each construct was fused to cYFP and expressed in leek epidermal cells along with nYFP-PEX7. A punctate fluorescent signal was observed only in cells co-expressing RabE1c[Q74L]-cYFP and nYFP-PEX7 (Figure 2.3C). The observed green punctate structures were the same as the structures identified as peroxisomes in cells expressing wild-type RabE1c-cYFP and nYFP-PEX7 (Figure 2.2A). No signal was detected in cells expressing either RabE1c[S29N]-cYFP and nYFP-PEX7 (Figure 2.3B) or RabE1c[N128I]-cYFP and nYFP-PEX7 (Figure 2.3D). These results indicate that GTP-bound RabE1c, but not GDP-bound RabE1c, interacts with PEX7.

GFP-PEX7 expression reduces peroxisomal β-oxidation, and RabE1c deficiency restores the effects of GFP-PEX7 in Arabidopsis

PEX7 is involved in various functions related to peroxisomal protein transport. Therefore, we assessed the involvement of the PEX7-binding protein RabE1c in peroxisome function. To analyze the physiological role of RabE1c, we used an Arabidopsis *rabe1c* knockout mutant. Peroxisomal fatty-acid β-oxidation is the main pathway for the catabolism of seed-reserved lipids. This pathway also converts 2,4-DB to 2,4-D, which inhibits root elongation at an early stage of seedling growth in Arabidopsis (Hayashi et al. 1998). Therefore, mutants with deficient peroxisomal β-oxidation are resistant to 2,4-DB but sensitive to 2,4-D (Hayashi et al. 1998). 2,4-DB sensitivity was evaluated by monitoring the seedling growth of *rabe1c* knockout plants. The root growth of *rabe1c* seedlings during germination was sensitive to 2,4-DB to an extent similar to that of wild-type plants (Figure 2.4). Peroxisomal fatty acid β-oxidation is responsible for the mobilization of seed-reserved lipid into sucrose in seedlings. Therefore, mutants with deficient peroxisomal β-oxidation require exogenously applied sucrose for successful

establishment of seedlings (Hayashi et al. 1998, Zolman et al. 2000). The *rabe1c* seedlings grew without sucrose as well as wild-type seedlings did (Figure 2.4). These findings indicate that peroxisomal fatty-acid β-oxidation is not impaired in the *rabe1c* mutant seedlings. Next, we examined the growth of GFP-PEX7–expressing plants (Figure 1.1B). In addition, we crossed *rabe1c* with GFP-PEX7 plants to generate GFP-PEX7/*rabe1c* plants, and the growth of these plants was examined under the same conditions. The GFP-PEX7 seedlings were resistant to 2,4-DB and required exogenous sucrose for germination (Figure 2.4A and 2.4B), indicating that the expression of GFP-PEX7 results in reduced peroxisomal β-oxidation activity. This finding suggests that GFP-PEX7 has a negative effect on peroxisome biogenesis. However, this phenotype was rescued by the *rabe1c* mutation in GFP-PEX7 plants, as demonstrated by the observation that GFP-PEX7/*rabe1c* seedlings were 2,4-DB–sensitive and sucrose-independent to a degree similar to wild-type plants (Figure 2.4A and 2.4B). This result shows that defective peroxisomal β-oxidation in GFP-PEX7 seedlings can be restored by the loss of RabE1c function.

GFP-PEX7 expression reduces peroxisomal protein transport, and RabE1c deficiency restores the peroxisomal protein transport, in GFP-PEX7 expressing plants

Because defective peroxisomal β-oxidation is often attributed to reduced transport of peroxisomal matrix enzymes, we measured the peroxisomal import of 3-ketoacyl-CoA thiolase, a PTS2-containing protein that catalyzes the last step of β-oxidation. Arabidopsis PTS2-containing proteins are synthesized in the cytosol as longer precursor peptides. After entry into peroxisomes, they are processed into their mature forms via the removal of their PTS2 sequences by the peroxisomal protease DEG15 (Schuhmann et al. 2008). Accumulation of the 3-ketoacyl-CoA thiolase precursor was detected in *pex7i* knockdown plants, as previously reported (Figure 2.5) (Hayashi et al. 2005). This thiolase precursor was not detected in the *rabe1c* mutant seedlings (Figure 2.5), indicating that the import of PTS2-containing proteins occurs normally in the absence of RabE1c. By contrast, a significant amount of thiolase

precursor was detected in the GFP-PEX7 seedlings (Figure 2.5), suggesting that the import of PTS2-containing proteins is reduced in these plants. These results were consistent with the defect in peroxisomal β-oxidation observed in the GFP-PEX7 plants (Figure 2.4). By contrast, almost no thiolase precursor was detected in the GFP-PEX7/*rabe1c* seedlings (Figure 2.5), indicating that the *rabe1c* mutation diminished the effect of GFP-PEX7 expression. This result was consistent with the rescue of peroxisomal β-oxidation in GFP-PEX7/*rabe1c* plants observed during germination (Figure 2.4).

Degradation of endogenous soluble PEX7 is dependent on RabE1c in the GFP-PEX7-expressing plants

Because PEX7 is responsible for the import of PTS2 proteins, we measured the expression levels of PEX7 protein in wild-type and mutant plants (Figure 2.5). The amount of endogenous PEX7 was the same in *rabe1c* and wild-type plants, but the level was reduced in GFP-PEX7 seedlings. This result indicates that expression of GFP-PEX7 protein reduces the level of endogenous PEX7, leading to reduced import of PTS2-containing proteins. However, endogenous PEX7 protein was restored to wild-type levels in the GFP-PEX7/*rabe1c* transgenic plants, indicating that RabE1c is involved in GFP-PEX7–induced reduction of PEX7. No significant difference in the level of GFP-PEX7 protein was observed between GFP-PEX7 and GFP-PEX7/*rabe1c* plants.

In Arabidopsis, PEX7 is mainly localized to the cytosol (Singh et al. 2009). To determine whether the reduction in PEX7 accumulation in GFP-PEX7 plants occurs in the cytosol, homogenates prepared from 5-day-old dark-grown seedlings were separated into soluble and membrane fractions by centrifugation at 100,000 × *g*. These fractions were then separated by SDS-PAGE and subjected to immunoblot analysis (Figure 2.6). Two peroxisomal proteins, thiolase and PEX14, were used as markers of soluble and membrane fractions, respectively (Hayashi et al. 1998 and 2000). As expected, thiolase and PEX14 were recovered in the soluble and membrane fractions, respectively, confirming that the fractionation technique was effective

(Figure 2.6). In wild-type plants, the majority of PEX7 was recovered in the soluble fraction (Figure 2.6). The *rabe1c* mutant exhibited a similar PEX7 level and accumulation pattern to that of wild-type plants (Figure 2.6). In the GFP-PEX7 plants, however, the PEX7 level was significantly reduced in the soluble fraction, whereas its level in the membrane fraction remained similar to that of wild-type plants, indicating a reduction in cytosolic PEX7. The level of soluble PEX7 was restored to that of wild-type plants in the GFP-PEX7/*rabe1c* transgenic plant, indicating that loss of RabE1c activity increased the cytosolic proportion of PEX7 in the GFP-PEX7 plants.

Surprisingly, in contrast to endogenous PEX7, the GFP-PEX7 fusion protein was abundant in the insoluble membrane fraction in both the GFP-PEX7 and GFP-PEX7/*rabe1c* seedlings (Figure 2.6). GFP-PEX7 protein levels were identical in these two types of seedlings in both the soluble and membrane fractions. These findings suggest that unlike PEX7, GFP-PEX7 is stacked on the peroxisomal membrane, and is not dislocated to the cytosol by its defective release from the peroxisomal membrane, in GFP-PEX7 and GFP-PEX7/*rabe1c* plants.

The proteasome is responsible for the degradation of endogenous PEX7 in GFP-PEX7 expressing plant

PEX7 is targeted to peroxisomes, and then dislocated into the cytosol in yeast and mammals (Mukai et al. 2002, Nair et al, 2004). In yeast, membrane binding of PEX7 requires the auxiliary proteins PEX18 and PEX20 (Einwachter et al. 2001, Purdue and Lazarow 2001). These auxiliary proteins are poly-ubiquitinated at the last step of dislocation, a modification that destines them for degradation via the 26S proteasome (Purdue and Lazarow 2001, Leon et al. 2006). However, it is not known whether PEX7 is degraded by the proteasome. To determine whether the reduction of PEX7 expression involves proteasome-mediated degradation in the GFP-PEX7 plants, we examined the effect of two proteasome inhibitors, MG132 and lactacystin. Seedlings were treated with either inhibitor for 3 h and homogenized, and PEX7 protein levels were determined by immunoblot analysis. As shown in Figure 2.7, the PEX7 protein level was significantly increased in GFP-PEX7 plants after proteasome-

inhibitor treatment, to a level comparable to that in GFP-PEX7/*rabe1c* plants. Neither inhibitor had any effect on the level of PEX7 in wild-type or *rabe1c* mutant plants, indicating that PEX7 is degraded by the proteasome in the presence of GFP-PEX7.

2.4 Discussion

Identification of PEX7 binding proteins by proteomic analysis

Previously, we showed that PEX7 can bind PEX5 in Arabidopsis (Nito et al. 2002, Singh et al. 2009). PEX7 contains a WD40 repeat, a sequence known to bind the T-complex, a cytosolic chaperonin (Valpuesta et al. 2002, Yi et al. 2006). During the course of this study, we identified PEX5 and all subunits of the T-complex as GFP-PEX7–associated proteins (Table 1.1). In addition to these known PEX7-binding proteins, we identified five new proteins as novel candidates for PEX7-binding proteins, including two small GTPases. Based on increasing evidence for the relationship between small GTPases and peroxisomes (Anthonio et al. 2009, Hotchin et al. 2010), we further investigated the involvement of these proteins in peroxisomal biogenesis. Although Arabidopsis Rab GTPases share highly similar amino-acid sequences, proteomic analysis identified only RabE1c and RabA1e as potential PEX7-binding proteins. The peroxisomal localization of RabE1c suggested that RabE1c interacts with PEX7 on the peroxisomal membrane. Consistent with this, we demonstrated that the *in vivo* interaction between PEX7 and RabE1c occurs on peroxisomes (Figure 2.2). GTP-bound active RabE1c, but not GDP-bound inactive RabE1c, can bind specifically to PEX7 (Figure 2.3), suggesting that RabE1c regulates PEX7 expression levels by binding to and dissociating from PEX7 during the GDP/GTP cycle.

RabE-type GTPase is a regulatory factor of peroxisomes

Rab GTPases are widely distributed across eukaryotic organisms and comprise eight subfamilies in Arabidopsis (Rutherford and Moore 2002). These Rab GTPases are involved primarily in membrane traffic, and most are localized to components of the secretory pathway (Woollard and Moore. 2008). However, some GTPases are involved not only in membrane traffic, but also in other cellular mechanisms. In mammals, RhoA, Rho kinase II, and Rab8a, a close homolog of Arabidopsis RabE1c, are associated with peroxisomes and cooperate in peroxisome-

cytoskeleton interactions (Hotchin et al. 2010). When we examined the subcellular localization of GFP-tagged AtRabE1c, we found that it partially localized to peroxisomes, suggesting that RabE1c is also involved in peroxisomal biogenesis in plants.

GFP-PEX7 expression decreases peroxisomal protein transport as a result of a reduction in the endogenous PEX7 level

After cargo release, PEX7 in yeast and mammalian cells is dislocated into the cytosol for the next round of import (Mukai et al. 2002, Nair et al. 2004). Therefore, PEX7 is localized predominantly in the cytosol in wild-type cells. We found, however, that the GFP-PEX7 fusion protein behaves significantly differently from endogenous PEX7. Cell-fractionation analysis revealed that PEX7 is present mainly in the soluble fraction, which presumably represents the cytosol, whereas GFP-PEX7 was mainly observed in the insoluble membrane fraction (Figure 2.6). These data suggest that release of GFP-PEX7 from the peroxisome is impaired, resulting in its accumulation in the membrane fraction. Similar phenomena have been reported in *S. cerevisiae* and mammalian cells, in which PEX7 tagged with either HA or GFP localizes to the peroxisome membrane (Zhang and Lazarow. 1995, Ghys et al. 2002), suggesting that tagged PEX7 cannot be dislocated from the peroxisome. We also found that expression of GFP-PEX7 has a dominant-negative effect on peroxisomal function: a defect in peroxisomal β-oxidation was observed in the GFP-PEX7-expressing plants (Figure 2.4), as was a defect in PTS2 protein import (Figure 2.5). This defect was accompanied by a reduction in the level of endogenous PEX7 (Figure 2.5) relative to the level in wild-type plants.

The mechanism by which GFP-PEX7 causes the degradation of endogenous PEX7 remains unclear. One potential explanation may be that the decrease in PEX7 accumulation is mediated by the quality-control system (Kiel et al. 2005). This system is illustrated by the fate of PEX5, a PTS1 receptor, in specific mutant backgrounds. In wild-type cells, PEX5 is normally dislocated into the cytosol upon mono-ubiquitination. However, in mutants defective in receptor dislocation,

such as *Pichia pastoris pex1*, *pex4*, *pex6*, *pex22*, human *pex1*, *pex6*, and Arabidopsis *pex6*, PEX5 accumulates in the peroxisome and becomes poly-ubiquitinated and targeted for subsequent degradation by the 26S proteasome (Koller et al. 1999, Zolman and Bartel 2004, Dodt and Gould 1996, Yahraus et al. 1996). In these mutants, PEX5 levels are depleted, thereby impairing the import of peroxisomal proteins. This type of quality-control may also operate for PEX7 degradation. We propose that high levels of membrane-stacked GFP-PEX7 stress the peroxisomal membrane, or GFP-PEX7 and PEX7 may dimerize with each other, leading both proteins to be recognized as targets for degradation. However, the observation that the level of GFP-PEX7 does not change suggests that GFP-PEX7 is resistant to degradation. It is possible that the GFP domain of GFP-PEX7 blocks the ubiquitination site in PEX7, which is responsible for both dislocation and proteasome-dependent degradation. Consistent with this, fusion of GFP to the C-terminus of PEX7 impairs its dislocation in yeast and mammalian cells (Nair et al. 2004, Ghys et al. 2002). In addition, another group has presented evidence that the fusion of a myc-tag to the N-terminus of PEX5 interferes with poly-ubiquitination and subsequent degradation (Platta et al. 2007). These results suggest that fused polypeptide tags interfere with the removal of transport receptors from the peroxisomal membrane.

PEX7 degradation depends on RabE1c

The simple *rabe1c* knockout mutant did not exhibit any peroxisomal defects, suggesting that *RabE1c* is dispensable for peroxisome function in the wild-type background, at least under our experimental conditions. However, we found that mutation of *rabe1c* reversed the defects in peroxisomal function and peroxisomal protein transport in the GFP-PEX7 background, suggesting that RabE1c is involved in the maintenance of PEX7 quality when abnormal PEX7 accumulates on the peroxisome membrane. A model outlining this mechanism is shown in Figure 2.8.

In GFP-PEX7 seedlings (Figure 2.8A), endogenous PEX7 is degraded via the 26S proteasome. In GFP-PEX7/*rabe1c* mutants (Figure 2.8B), even though the same amount of GFP-PEX7 protein accumulates on the peroxisomal membranes as in

GFP-PEX7 plants, endogenous PEX7 is restored almost to the level in wild-type plants (Figure 2.5). Therefore, RabE1c is responsible for the degradation of endogenous PEX7 in the presence of GFP-PEX7. The protein level of soluble PEX7 was restored in the GFP-PEX7/*rabe1c* mutant seedlings (Figure 2.6), suggesting that RabE1c dysfunction increases cytosolic PEX7 in the GFP-PEX7 background. In addition, PTS2-containing protein import (Figure 2.5) and peroxisomal β-oxidation (Figure 2.4) were restored. Thus, endogenous cytosolic PEX7, rather than membrane-bound GFP-PEX7, is essential for transport of PTS2-containing proteins.

A recent study showed that the degradation of the import machinery residing on the outer membrane of plastids occurs in the plastid outer membrane and is regulated by a ubiquitin E3 ligase (Ling et al. 2012). In our study, we identified RabE1c as a novel PEX7-binding protein involved in targeting PEX7 for degradation when abnormal PEX7 is present on the peroxisomal membrane. Our findings also demonstrate that our proteomic analysis can specifically and effectively identify new regulatory components, and highlight the potential utility of performing similar experiments to examine the regulation of other PEXs.

Chapter 3

Functional characterization of two novel proteins that bind PEX16

3.1 Introduction

Genetic and biochemical studies in yeast and mammlian cell systems have led to the identification of three peroxisomal membrane proteins (PMPs), PEX3, PEX16 and PEX19, that are specifically involved in peroxisomal membrane protein transport (Heiland and Erdmann 2005). The peroxisomes are absent when any one of these proteins are mutated or absent. Defect of the function of these proteins is causal for Zellweger syndrome, a lethal disease that occurs in human. PEX3 is an integral peroxisomal membrane protein that acts as a docking receptor for incoming peroxisomal membrane proteins, including PEX19 (Fang et al. 2004). PEX16, an integral peroxisomal membrane protein, is thought to serve as a receptor for PEX3 in the ER (Honsho et al. 2002) and thus acts in the most upstream of peroxisomal formation from ER. PEX16 is absent in most yeast except for *Yarrowia lipolitica*, in which it has an additional role in peroxisomal morphology.

In Arabidopsis, it is believed that all of these proteins are essential for plant survival, basically because all the attempts to isolate homozygous lines for the knockout mutants of these PEX proteins have been failed, including PEX16. The lack of information in their knockout mutants has led for several questions including: whether peroxisomes are formed from the ER in plants? whether peroxisomal proteins traffics through the ER to peroxisomes? whether and how PEX16 regulates this pathway if ER is involved in peroxisomal formation?

Karnik and Trelease (2005) showed that PEX16 coexists in the ER and peroxisomes in Arabidopsis cultured cells. In addtition, Arabidopsis PEX16 could partially complement the growth of *pex16* mutant of the yeast *Yarrowia lipolitica* on oleic acid as sole carbon source, even though the sequence similarity of PEX16 between Arabidopsis and Yarrowia is low (26%) (Lin et al, 1999). These studies raise the possibility and the importance of Arabidopsis PEX16 for peroxisomal formation via the ER. In Arabiodopsis, it was shown that GFP-PEX16 is localized on peroxisomes and the overexpression of GFP-PEX16 induces peroxisomal aggregation

(Lin et al. 2004). In addition, suppression of PEX16 by RNAi produces enlarged but fewer peroxisomes within the cell (Nito et al. 2007). These indicate that PEX16 also regulates the positioning and morphology of peroxisomes in Arabidopsis. Understanding the binding proteins of PEX16 and their functions may provide an insight into the regulatory mechanism of PEX16 for peroxisomal biogenesis. Two proteins, PBP1 and PBP2, were identified as novel binding partners of PEX16 in our attempts to isolate PEX16 complex, in Chapter 1. In this chapter, I describe the mutant analysis of *pbp1* and *pbp2*.

3.2 Materials and methods

Plant materials

Arabidopsis thaliana ecotype Columbia was used as wild-type plants. *pbp1* and *pbp2* are GT (CS176233) line with Landsberg erecta background and SAIL (CS831290) line with Columbia background, respectively. They were obtained from ABRC.

Establishment of plant strains

pbp1 mutant carries a single *Ds* transposon in the *At5g10890* gene. *pbp2* mutant carries T-DNA in the *At5g06350* gene. The position of each insertion was confirmed by PCR using *PBP1* and *PBP2* specific primers spanning the inserted regions and further confirmed by Ds transposon and T-DNA specific primers. The forward and reverse primers specific for *PBP1* were originally attached with *attB1* and *attB2*, respectively. The homozygous plants of GFP-PTS1/*pbp1* and GFP-PEX16/*pbp1* were generated by crossing *pbp1* with GFP-PTS1 and GFP-PEX16 respectively, of which homozygote for *pbp1* was confirmed by PCR indicated above in F2 generation and for transgenes confirmed by segregation pattern in F3 generation.

Nucleotide sequences of primers used for PCR to check T-DNA insertion position are as follows.

• For *pbp1*

5G10890-F: 5’-AAAAAGCAGGCTCTATGGCGGAACCAAGGGTGAG-3’

5G10890-R+S: 5’-AGAAAGCTGGGTCTCACCTTGAGAGAGGGTAAGG-3’

GT line Ds5O: 5’-GTTCGAATTCGATCGGGATAAAAC-3’

• For *pbp2*

5G06350-N0: 5’-TTGTTTCCGTTCTTCCGCC-3’

5G06350-R567: 5’-AGCATCCAAGGAAAAGGTAG-3’

SAIL LB1: 5’-GCCTTTTCAGAAATGGATAAATAGCCTTGCTTCC-3’

Plant growth conditions

The composition of growth medium and the condition for seed germination and plant growth was described previously in Chapter 1. The growth medium for the incubation of leek epidermal cells that were used in transient expression experiments was the same as the one for Arabidopsis seedlings.

Confocal laser scanning microscopic observation

The experimental procedure was the same as that in Chapter 2.

Plasmid construction

The cDNA fragments of *PEX16*, *PBP1* and *PBP2* were conjugated with *attB1* and *attB2* at their 5' and 3' ends, respectively, and amplified by PCR with gene specific primer sets and cloned into the entry vector, pDONR221, using the Gateway BP recombination method (Invitrogen).

To construct GFP-, tdTomato- and -GFP fusion proteins, the cDNAs that were cloned into pDONR221 were transferred into the destination vector, p2FGW7 (Invitrogen) to generate GFP- fusion, into ptdGW (Kindly provided by Dr. Mano; National Institute for Basic Biology) to generate tdTomato-fusion, or into p2GWF7 to generate -GFP fusion, using Gateway LR recombination reaction.

Nucleotide sequences of primers used for the amplification of genes in this method are as follows.

• For PEX16 cloning destined to p2FGW7

2G45690 F: 5'-AAAAAGCAGGCTCAATGGAAGCTTATAAGCAATG-3'

2G45690 R+: 5'-AGAAAGCTGGGTCTCACGATCCCGATATGTAAGT-3'

•For PEX16 cDNA cloning destined to p2GWF7

2G45690 F: 5'-AAAAAGCAGGCTCAATGGAAGCTTATAAGCAATG-3'

2G45690 R-: 5'-AGAAAGCTGGGTACGATCCCGATATGTAAGTGTAC-3'

•For PBP1 cDNA cloning destined to p2FGW7 and ptdGW

5G10890-F: 5'-AAAAAGCAGGCTCTATGGCGGAACCAAGGGTGAG-3'

5G10890-R+S: 5’-AGAAAGCTGGGTCTCACCTTGAGAGAGGGTAAGG-3’

•For PBP1 cDNA cloning destined to p2GWF7

5G10890-F: 5’-AAAAAGCAGGCTCTATGGCGGAACCAAGGGTGAG-3’

5G10890-R-S; 5’-AGAAAGCTGGGTACCTTGAGAGAGGGTAAGGATG-3’

•For PBP2 cDNA cloning destined to p2FGW7

5G06350-F: 5’-AAAAAGCAGGCTATATGGTTCGCTCCAAGGCTC-3’

5G06350-R+S: 5’-AGAAAGCTGGGTATTACGCGAGTAAGCTTTTGGA-3’

•For PBP2 cDNA cloning destined to p2GWF7

5G06350-F: 5’-AAAAAGCAGGCTATATGGTTCGCTCCAAGGCTC-3’

5G06350-R-S: 5’-AGAAAGCTGGGTACGCGAGTAAGCTTTTGGAC-3’

Transient expression in leak epidermal cells

For particle bombardment-mediated CaMV35S-driven transient expression, the plasmids of p2FGW7, p2GWF7 and ptdGW containing cDNAs of *PEX16* or *PBP1* were coated onto gold particles of 1.0 μm in diameter and bombarded into leek epidermal cells using the PDS-1000/He Biolistic Particle Delivery System (Bio-Rab) followed by incubation under dark condition. For the detection of colocalization, GFP-PEX16 and tdTomato-PBP1 were simultaneously coated on the same gold particles for the subsequent expression.

3.3 Results

Analysis of PBP1 function for its involvement in peroxisomal morphogenesis and positioning

PBP1 was identified as one of the PEX16 binding proteins by coimmunoprecipitation (in Chapter 1). According to TAIR website (http://www.arabidopsis.org), it is annotated as a protein containing myosin a heavy chain-related domain with its biological functions unknown. To examine its subcellular localization, the fusion protein with GFP tagged to either N (GFP-PBP1) or C terminus (PBP1-GFP) of CDS of PBP1 was transiently expressed in leek epidermal cells (Figure 3.1). Both GFP-PBP1 and PBP1-GFP were localized in the cytosol and tubular structures without any peroxisomal structures. However, when PEX16 and PBP1 proteins were coexpressed, PBP1 showed high accumulation on the aggregated peroxisomes (Figure 3.2), indicating that PEX16 recruits PBP1 to peroxisomal membranes where they make interaction.

We previously suppressed *PEX16* expression by introducing RNA interference of PEX16 into GFP-PTS1 transgenic plants to visualize peroxisomes (Nito et al. 2007). As a result, peroxisomes became enlarged to approximately 5-10 times in *pex16i* plant compared to those in wild-type plants, suggesting that PEX16 controls morphology of peroxiosmes. The position of peroxisomes are also regulated by PEX16 as we found previously that GFP-PEX16 overexpression alters the special distribution of peroxisomes by forcing the dispersed peroxisomes into a single aggregates (data not shown). Since PBP1 is a binding protein of PEX16, I expected that it may be also involved in the similar function for peroxisomes. To examine this hypothesis, the *pbp1* knockout mutant was analyzed to observe its effect on peroxisomal morphology and positioning (Figure 3.3A). *pbp1* mutant was crossed with GFP-PTS1 overexpressing plant to visualize the peroxisomes. As shown in Figure 3.3C, the number and size of the peroxisomes in *pbp1* are almost identical to those in the wild-type plants (Figure 3.3B), indicating that the defect of PBP1 does not affect peroxisomal morphology. *pbp1* mutant was also crossed with GFP-PEX16

overexpressing plant to see whether it is involved in the peroxisomal aggregation process. As shown in Figure 3.3D and 3.3E, peroxisomal aggregates were appeared almost identically between wild-type and *pbp1* mutant, indicating that the defect of PBP1 has no effect on the GFP-PEX16 induced peroxisomal accumulation. In addition, *pbp1* did not display any defect on peroxisomal protein transport and β-oxidation.

Taken together, these data suggest that PBP1 may not have similar function of PEX16 even though it interacts with PEX16, or its function on peroxisomes is compensated by other redundant proteins. Recently, it is found that Arabidopsis has a homologous protein (At4g31805) of PBP1. Even though they have low sequence similarity in total amino acids (23%), they have highly conserved N-terminal domain (Figure 3.3F). Based on the Blast search in NCBI database (http://www.ncbi.nlm.nih.gov), I found that three motifs that are highly conserved in their N-terminal regions (Figure 3.3F) are conserved in other plant species. It suggests that PBP1 and At4g31805 may have a redundant function on peroxisomal positioning and morphology, with their N-terminal domain being involved.

The mutant analysis of PBP2

PBP2 is another binding protein of PEX16 in addition to PBP1 (in Chapter 1), which contains a domain with an armadillo like fold. This domain is known to have binding capacity to large proteins and is found in various proteins with different functions. To investigate the biological function of PBP2, Arabidopsis *pbp2* mutant was analyzed (Figure 3.4). However, in the early attempt to isolate the knockout mutants of *pbp2*, I failed to generate the homozygous lines by selfing the heterozygous plants, as shown in Figure 3.4B and 3.4C that heterozygous *pbp2* produces about 25% of the aborted seeds in the fruits, suggesting that homozygous mutant is lethal during early seed development. The localization of PBP2 was not clear because the chimeric protein of PBP2 fused with GFP was not expressed in all the experiments conducted. Therefore, the function of PBP2 is still unclear.

3.4 Discussion

As peroxisomes are dynamic organelles in plants, their matrix components, numbers and morphologies should be strictly regulated to cooperate cell metabolism to different developmental stages and various environmental conditions. Compared to *pex16* knockout mutant, which is lethal, *pex16i* mutant was appeared to be viable and displayed enlarged peroxisomes within the cells (Nito et al. 2007), suggesting that PEX16 is not only important for plant development but also required for the maintenance of the morphology of peroxisomes. GFP-PEX16 overexpression induces the aggregation of peroxisomes suggesting that PEX16 is also involved in the positioning of peroxisomes. We previously found that actin filament mediates this PEX16-mediated aggregation (data not shown). Wiemer et al. (1997) reported the formation of large peroxisomal aggregates in living mammalian cells treated with the microtubule-destabilizing drug nocodazole, indicating the requirement of microtubules for maintaining the spatial distribution of peroxiomes. On the other hand, plant uses actin filament instead of microtubule for peroxisomal movement and thus the positioning as well (Jedd and Chua 2002), suggesting that there is a functional relationship between actin filament and PEX16 protein on peroxisomal aggregation. This led us to speculate that PBP1 and PBP2 functions on peroxisomal movements, probably by mediating the physical association between peroxisomes and actin filaments through PEX16 binding. Alternatively, it is expected that they control the morphology of peroxisomes based on the phenotype of enlarged peroxisomes in *pex16i* plants.

The colocalization of PBP1 and PEX16 in peroxisomes (Figure 3.2) shows that PBP1 is a component of the PEX16 regulatory machinery and may functionally associated with PEX16. However, the suppression of PBP1 did not alter either peroxisomal morphology (Figure 3.3C) or accumulation (Figure 3.3E) compared to wild-type, suggesting that PBP1 protein is either dispensable for peroxisomal morphology and special distribution, or there is a functionally redundant protein in Arabidopsis. PBP1 actually has a homolog with highly conserved N-terminal domain,

that is likely to be plant-specific, suggesting that the later possibility is higher. There is complete lack of information about the PBP2 protein, and since *pbp2* mutant shows lethality during seed development, the function of PBP2 protein is not yet clear in terms of peroxisomal biogenesis. However, as both *pbp2* and *pex16* knockout mutants are lethal during seed development, it raises a speculation that PBP2 is functionally associated with and as essential for plant growth as PEX16.

What roles do PBP1 and PBP2 play on the function of peroxisomes? Do they regulate PEX16 function and how? Our results could not answer these questions at this moment except for their binding activity with PEX16 and possible involvement in peroxisomal biogenesis. However, it will be interesting to determine whether PBP1 and PBP1 homolog (At4g31805) are redundantly involved in peroxisomal biogenesis by analyzing the double knockout mutants in Arabidopsis. In addition, analysis of RNAi knockdown mutant that suppresses PBP2 expression may provide information on its function. Taken together, further experiments are required to answer the function of PBP1 and PBP2 on peroxisomes and the molecular mechanism of their machinery controlling the peroxisomal structure, positioning and movement.

General discussion

Recent advances in mass spectrometry based proteomic approaches combined with a wide range of biochemical experiments have improved the way of identifying novel peroxisomal proteins, thus discovering novel functions of peroxisomes (Reumann et al. 2007 and 2009, Arai et al. 2008). Although these classical methods of peroxisomal isolation are dedicated to high-throughput identification of peroxisomal proteins, it is technically comprehensive and requires a large investment of time. The unavoidable contamination of other organelles is also typical hurdles towards the detection of peptides of peroxisomal proteins by mass analysis. This study provided a rapid, efficient and highly selective approach for the identification of novel factors that are involved in peroxisomal biogenesis.

In the nature, most proteins exist as protein complexes and it reflects the importance of the protein-protein interactions for biological functions within the cells. It prompted us to isolate the protein complex containing PEX7, a receptor for peroxisomal matrix protiens, and PEX16, a peroxisomal membrane protein involved in the structure and positioning of peroxisomes. Identification of the binding proteins of PEX7 and PEX16 therefore provides us the important knowledge on the transport machinery across the peroxisomal membranes and the machinery controlling peroxisomal membrane dynamics, respectively.

In our study, the implication of molecular chaperonins on peroxisomal functions was described. Four peroxisomal chaperone proteins, DEG15, LON2, HSP15.7 and ACD31.2, have been reported in plant (Ma et al. 2006, Schuhmann et al. 2008, Lingard and Bartel 2009). They all contain PTS1 or PTS2 in their peptides and are localized to peroxisomes. Therefore, their functions on the maintenance of peroxisomal proteins take place within peroxisomes. In comparison to these chaperones, the isolation of a cytosolic chaperonin (T-complex) and chaperone (CPN60B) as PEX7-binding proteins in our study suggests the requirement of cytosolic chaperons in peroxisomal protein transport in plant. Since the binding between PEX5 and PEX7 in the cytosol (Singh et al, 2009) is required for PEX7-mediated PTS2 import into peroxisomes (Woodward et al, 2005), it is tempting to speculate that T-complex may stabilize PEX7 and PEX5 to facilitate the PTS2 import.

Alternatively, T-complex and PEX5 may competitively bind to PEX7 because of the facts that PEX5 binds to PEX7 through WD-40 repeats within PEX7 (Nito et al. 2002) and T-complex binds to the WD-40 motif in mammalian cells (Yi et al. 2006). Therefore, it is assumed, in this case, that T-complex may control the efficiency of PEX7-mediated PTS2 protein transport by acting as a suppressor for PEX7 import against PEX5, which act as a facilitator for PEX7 import. The absence of or the failure of our attempts at getting the knockout mutants of the T-complex subunits might be due to the pleiotropic functions of T-complex. It should be noted that each subunit of T-complex has been shown to have different binding substrates (Llorca et al. 1999, Amit et al. 2010, Nadler et al. 2012). Therefore, our study raises interesting questions for next mission that which subunits and through what mechanism T-complex binds to PEX7 to regulate the import of peroxisomal matrix proteins for plant growth and development. In future, further solid evidence for these questions needs to be provided by creation of transgenic plants expressing RNAi for each T-complex subunit and structural study of the responsible subunit for PEX7 interaction.

Our study on PEX7-binding proteins also implies a role for RabE1c in the degradation of PEX7 for the regulation of abnormal PEX7. This might be important during certain stress conditions in which peroxisomal receptors become damaged and accumulated on the peroxisomal membranes. For example during seedling germination or under strong light condition in which massive amount of H_2O_2 are produced within peroxisomes. In Arabidopsis, it was reported that during seedling germination when peroxisomes and oil bodies make close proximity, H_2O_2 produced within peroxisomes as a by-product of fatty acid β-oxidation can damage the oil body membrane-residing SDP1 protein if H_2O_2 is not properly removed (Eastmond 2007). Considering this, it is reasonable to expect that the peroxisomal proteins are also confronting H_2O_2-caused damage during plant growth. The recycling of PEX7 and PEX5 is challenged in this case since these receptors may loose the activities for recycling and accumulated on peroxisomes. In yeast, it was shown that the removal of PEX5 that is accumulated on peroxisomal membranes is essential to initiate the import of newly synthesized PEX5 and therefore to ensure the cargo import for

sustained peroxisomal functions (Dodt and Gould. 1996, Yahraus et al. 1996). This kind of receptor controlling system is so called quality control system and can be applied to PEX7 as well. Identification of RabE1c as the novel protein involved in the quality control system of PEX7 extends our knowledge for the existence of this quality system in plants and gives new insight into the mechanism of PEX7 regulation during dislocation from peroxisomes. Although the degradation of PEX7 was not found during germination we tested, further experiments should be required to determine what kind of stresses particularly damage PEX7 and thus necessitate RabE1c involvement in PEX7 regulation for normal peroxisomal function and plant growth. Considering RabE1c is also conserved among organisms, its similar role on peroxisomal function especially for PEX7 dislocation is expected in other organisms and provides a new insight into the study of receptor recycling pathway for peroxisomal biogenesis.

Our initial purpose of studying PEX16 is to understand whether peroxisomes are formed from ER and whether PEX16 is involved in peroxisomal membrane protein transport from ER to peroxisomes. PEX16 is N-glycosylated (Titorenko and Rachubinski 1998), a modification site that occurs only in the ER, and thus is localized in the ER and peroxisomes in yeast, mammalian and Arabidopsis cultured cells (Honsho et al. 2002, Karnik and Trelease 2005). However, the ER localization of PEX16 has yet been reported in Arabidopsis plant so far, as is the case in our experiment in which GFP-PEX16 protein was only observed in peroxisomes. One explanation for this is that PEX16 protein transiently targets to the ER before its final destination on peroxisomes, which may result in its subcellular localization being observed only in peroxisomes. It is also likely that PEX16 stays in the ER in the manner of stage dependent, i.e. at early stage of embryo development at which it is assumed, yet poorly understood, that peroxisomes are *de novo* synthesized from ER. Further experiment should be carried out for the observation of GFP-PEX16 localization in various stages. However, it is still remained as a big argument that whether plant shares the same feature for the ER associated origin of peroxisomes. Since there is lack of solid data showing the ER-localized peroxisomal membrane

proteins or any mutant showing the accumulation of peroxisomal proteins on ER or ER-like structures in plant, the involvement of PEX16 in the *de novo* synthesis of peroxisomes should be carefully concerned.

On the other hand, previous studies in Arabidopsis showed that PEX16 is involved in the morphogenesis and positioning of peroxisomes. It is in lines with the function of PEX16 in yeast that overexpression of PEX16 induces fewer but enlarged peroxisomes (Eitzen et al. 1997). In mammalian cells, ER-localized Sec16A and Sec16B were recently identified as regulators for PEX16 sorting from ER to peroxisomes (Yonekawa et al. 2011), although the interaction between them was not shown. The depletion of Sec16B resulted in the elongation of peroxisomes, due to insufficient targeting of PMPs including PEX16 to peroxisomes. The role of PEX16 as well as its cofactors is still unclear so far in plant. Our study provided two candidate proteins for PEX16 regulation. Analysis of transgenic plants suppressing these genes and determination of the precise distribution of these proteins may shed light on the mechanism underlying the morphological and spacial changes of peroxisomes by PEX16 and may provide basic understanding for the involvement of PEX16 on PMP targeting to peroxisomes from ER.

Furthermore, this study highlights its application to study other peroxisomal proteins. Except for PEX7 and PEX16, Arabidopsis genome encodes additional 20 PEXs (PEX1, PEX2, PEX3A, PEX3B, PEX4, PEX5, PEX6, PEX10, PEX13, PEX11A, PEX11B, PEX11C, PEX11D, PEX11E, PEX12, PEX14, PEX15, PEX19A, PEX19B, PEX22) involving in peroxisomal biogenesis (Charlton and Lopez, 2002). The functions of some PEXs were characterized based on mutant analysis. However, none of them except PEX5 were tested for their associated proteins. Identification and characterization of the binding proteins of each PEX using this proteomic approach may provide us additional information on the novel peroxisomal biogenesis regulators and be helpful to dissect each part of peroxisomal biogenesis.

References

Anthonio EA, Brees C, Baumgart-Vogt E, Hongu T, Huybrechts SJ, Van Dijck P, Mannaerts GP, Kanaho Y, Van Veldhoven PP, Fransen M (2009) Small G proteins in peroxisome biogenesis: the potential involvement of ADP-ribosylation factor 6. BMC Cell Biol. 10: 58

Amit M, Weisberg SJ, Nadler-Holly M, McCormack EA, Feldmesser E, Kaganovich D, Willison KR, Horovitz A (2010) Equivalent mutations in the eight subunits of the chaperonin CCT produce dramatically different cellular and gene expression phenotypes. J. Mol. Biol. 401: 532-543

Arai Y, Hayashi M, Nishimura M (2008) Proteomic identification and characterization of a novel peroxisomal adenine nucleotide transporter supplying ATP for fatty acid β-oxidation in soybean and Arabidopsis. Plant Cell 20: 3227-3240

Braverman N, Dodt G, Gould SJ, Valle D (1998) An isoform of Pex5p, the human PTS1 receptor, is required for the import of PTS2 proteins into peroxisomes. Hum. Mol. Genet. 7: 1195-1205

Charlton W, Lopez HE (2002) PEX genes in plants and other organisms. In Plant Peroxisomes, A. Baker, and I.A. Graham, eds (Dordrecht, The Netherlands: Kluwer Academic Publishers), pp. 385–426.

Dodt G, Gould SJ (1996) Multiple PEX genes are required for proper subcellular distribution and stability of Pex5p, the PTS1 receptor: Evidence that PTS1 protein import is mediated by a cycling receptor. J. Cell Biol. 135: 1763-1774

Eastmond PJ (2007) MONODEHYROASCORBATE REDUCTASE4 is required for seed storage oil hydrolysis and postgerminative growth in arabidopsis. Plant Cell 19: 1376-1387

Einwachter H, Sowinski S, Kunau WH, Schliebs W (2001) *Yarrowia lipolytica* Pex20p, *Saccharomyces cerevisae* Pex18p/Pex21p and mammalian Pex5pL

fulfill a common function in the early steps of the peroxisomal PTS2 import pathway. EMBO Rep. 2: 1035–1039.

Eitzen GA, Szilard RK, Rachubinski RA (1997) Enlarged peroxisomes are present in oleic acid-grown *Yarrowia lipolytica* overexpressing the PEX16 gene encoding an intraperoxisomal peripheral membrane peroxin. J. Cell Biol. 137: 1265-1278

Erdmann R, Blobel G (1995) Giant peroxisomes in oleic acid-induced *Saccharomyces cerevisiae* lacking the peroxisomal membrane protein Pmp27p. J. Cell Biol. 128: 509-523

Faber KN, Heyman JA, Subramani S (1998) Two AAA family peroxins, PpPex1p and PpPex6p, interact with each other in an ATP-dependent manner and are associated with different subcellular membranous structures distinct from peroxisomes. Mol. Cell Biol. 18: 936-943

Fang Y, Morrell JC, Jones JM, Gould SJ (2004) PEX3 functions as a PEX19 docking factor in the import of class I peroxisomal membrane proteins. J. Cell Biol. 164: 863-875

Fransen M, Amery L, Hartig A, Brees C, Rabijns A, Mannaerts GP, Van Veldhoven PP (2008) Comparison of the PTS1- and Rab8b-binding properties of Pex5p and Pex5Rp/TRIP8b. Biochim. Biophys. Acta. 1783: 864-873

Fujimoto M, Arimura SI, Nakazono M, Tsutsumi N (2008) Arabidopsis dynamin-related protein DRP2B is co-localized with DRP1A on the leading edge of the forming cell plate. Plant Cell 27: 1581-1586

Ghys K, Fransen M, Mannaerts GP, Van Velhoven PP (2002) Functional studies on human Pex7p: subcellular localization and interaction with proteins containing a peroxisome-targeting signal type 2 and other peroxins. Biochem. J. 365: 41-50

Goto S, Mano S, Nakamori C, Nishimura M (2011) Arabidopsis ABERRANT PEROXISOME MORPHOLOGY9 Is a Peroxin That Recruits the PEX1-PEX6 Complex to Peroxisomes. Plant Cell 23: 1573-1587

Hayashi M, Aoki M, Kato A, Kondo M, Nishimura M (1996) Transport of chimeric proteins that contain a carboxy-terminal targeting signal into plant microbodies. Plant J. 10: 225-234

Hayashi M, Nito K, Toriyama-Kato K, Kondo M, Yamaya T, Nishimura M (2000) AtPex14p maintains peroxisomal functions by determining protein targeting to three kinds of plant peroxisomes. EMBO J. 19: 5701–5710.

Hayashi M, Toriyama K, Kondo M, Nishimura M (1998) 2,4-Dichlorophenoxybutyric acid-resistant mutants of Arabidopsis have defects in glyoxysomal fatty acid beta-oxidation. Plant Cell 10: 183-195

Hayashi M, Yagi M, Nito K, Kamada T, Nishimura M (2005) Differential contribution of two peroxisomal protein receptors to the maintenance of peroxisomal functions in Arabidopsis. J. Biol. Chem. 280: 14829-14835

Heiland I, Erdmann R (2005) Biogenesis of peroxisomes. Topogenesis of the peroxisomal membrane and matrix proteins. FEBS J. 272: 2362-2372

Hino T, Tanaka Y, Kawamukai M, Nishimura K, Mano S, Nakagawa T (2011) Two Sec13p homologs, AtSec13A and AtSec13B, redundantly contribute to formation of COPII transport vesicles in Arabidopsis thaliana. Biosci. Biotechnol. Biochem. 75: 1848-1852

Honsho M, Hiroshige T, Fujiki Y (2002) The membrane biogenesis peroxin Pex16p. Topogenesis and functional roles in peroxisomal membrane assembly. J. Biol. Chem. 277: 44513-44524

Hotchin NA, Schollenberger L, Gronemeyer T, Huber CM, Lay D, Wiese S, Meyer HE, Warscheid B, Saffrich R, Peränen J, Gorgas K, Just WW (2010) RhoA Regulates Peroxisome Association to Microtubules and the Actin Cytoskeleton. PLoS One 5: e13886

Jedd G, Chua NH (2002) Visualization of peroxisomes in living plant cells reveals acto-myosin-dependent cytoplasmic streaming and peroxisome budding. Plant Cell Physiol. 43: 384-392

Kamada T, Nito K, Hayashi H, Mano S, Hayashi M, Nishimura M (2003) Functional differentiation of peroxisomes revealed by expression profiles of

peroxisomal genes in *Arabidopsis thaliana*. Plant Cell Physiol. 44(12): 1275–1289

Kamada NT, Hayashi M, Fukazawa M, Sakakibara H, Nishimura M (2008) A putative peroxisomal polyamine oxidase, AtPAO4, is involved in the polyamine catabolism in Arabidopsis thaliana. Plant Cell Physiol. 49:1272-1282.

Kamigaki A, Kondo M, Mano S, Hayashi M, Nishimura M (2009) Suppression of peroxisome biogenesis factor 10 reduces cuticular wax accumulation by disrupting the ER network in *Arabidopsis thaliana*. Plant Cell Physiol. 50: 2034-2046

Karnik SK, Trelease RN (2005) Arabidopsis peroxin 16 coexists at steady state in peroxisomes and endoplasmic reticulum. Plant Physiol. 138: 1967-1981

Karnik SK, Trelease RN (2007) Arabidopsis peroxin 16 trafficks through the ER and an intermediate compartment to pre-existing peroxisomes via overlapping molecular targeting signals. J. Exp. Bot. 58: 1677-1693

Kato A, Hayashi M, Takeuchi Y, and Nishimura M (1996) cDNA cloning and expression of a gene for 3-ketoacyl-CoA thiolase in pumpkin cotyledons. Plant Mol. Biol. 31: 843–852.

Kiel JA, Emmrich K, Meyer HE, Kunau WH (2005) Ubiquitination of the peroxisomal targeting signal type 1 receptor, Pex5p, suggests the presence of a quality control mechanism during peroxisomal matrix protein import. J. Biol. Chem. 280: 1921-1930

Koller A, Snyder WB, Faber KN, Wenzel TJ, Rangell L, Keller GA, Subramani S (1999) Pex22p of *Pichia pastoris*, essential for peroxisomal matrix protein import, anchors the ubiquitin-conjugating enzyme, Pex4p, on the peroxisomal membrane. J. Cell Biol. 146: 99-112

Kragler F, Lametschwandtner G, Christmann J, Hartig A, Harada JJ (1998) Identification and analysis of the plant peroxisomal targeting signal 1 receptor NtPEX5. Proc. Natl. Acad. Sci. U S A 95: 13336-13341

Kubota H, Hynes G, Carne A, Ashworth A, Willison K (1994) Identification of six Tcp-1-related genes encoding divergent subunits of the TCP-1-containing chaperonin. Curr. Biol. 4: 89-99

Leon S, Zhang L, McDonald WH, Yates J, 3rd, Cregg JM, Subramani S (2006) Dynamics of the peroxisomal import cycle of PpPex20p: ubiquitin-dependent localization and regulation. J. Cell Biol. 172: 67-78

Lewis VA, Hynes GM, Dong Z, Saibil H, Willison K (1992) T-Complex Polypeptide-1 Is a Subunit of a Heteromeric Particle in the Eukaryotic Cytosol. Nature 358: 249-252

Lin Y, Cluette-Brown JE, Goodman HM (2004) The peroxisome deficient Arabidopsis mutant *sse1* exhibits impaired fatty acid synthesis. Plant Physiol. 135: 814-827

Lin Y, Sun L, Nguyen LV, Rachubinski RA, Goodman HM (1999) The Pex16p homolog SSE1 and storage organelle formation in Arabidopsis seeds. Science 284: 328-330

Ling Q, Huang W, Baldwin A, Jarvis P (2012) Chloroplast biogenesis is regulated by direct action of the ubiquitin-proteasome system. Science 338: 655-659

Lingard MJ, Bartel B (2009) Arabidopsis LON2 is necessary for peroxisomal function and sustained matrix protein import. Plant Physiol. 151: 1354-1365

Lingard MJ, Trelease RN (2006) Five Arabidopsis peroxin 11 homologs individually promote peroxisome elongation, duplication or aggregation. J. Cell Sci. 119: 1961-1972

Lingner T, Kataya AR, Antonicelli GE, Benichou A, Nilssen K, Chen XY, Siemsen T, Morgenstern B, Meinicke P, Reumann S (2011) Identification of novel plant peroxisomal targeting signals by a combination of machine learning methods and in vivo subcellular targeting analyses. Plant Cell 23: 1556-1572.

Llorca O, McCormack EA, Hynes G, Grantham J, Cordell J, Carrascosa JL, Willison KR, Fernandez JJ, Valpuesta JM (1999) Eukaryotic type II

chaperonin CCT interacts with actin through specific subunits. Nature 402: 693-696

Ma C, Haslbeck M, Babujee L, Jahn O, Reumann S (2006) Identification and characterization of a stress-inducible and a constitutive small heat-shock protein targeted to the matrix of plant peroxisomes. Plant Physiol. 141: 47-60

Mano S, Nakamori C, Hayashi M, Kato A, Kondo M, Nishimura M (2002) Distribution and characterization of peroxisomes in Arabidopsis by visualization with GFP: Dynamic morphology and actin-dependent movement. Plant Cell Physiol. 43: 331–341.

Mano S, Nakamori C, Kondo M, Hayashi M, Nishimura M (2004) An Arabidopsis dynamin-related protein, DRP3A, controls both peroxisomal and mitochondrial division. Plant J. 38: 487-498.

Marshall PA, Krimkevich YI, Lark RH, Dyer JM, Veenhuis M, Goodman JM (1995) Pmp27 promotes peroxisomal proliferation. J. Cell Biol. 129: 345-355

Matsumura T, Otera H, Fujiki Y (2000) Disruption of the interaction of the longer isoform of Pex5p, Pex5pL, with Pex7p abolishes peroxisome targeting signal type 2 protein import in mammals. Study with a novel Pex5-impaired Chinese hamster ovary cell mutant. J. Biol. Chem. 275: 21715-21721

Moser HW, Begin A, Cornblath D (1991) Peroxisomal disorders. Biochem. Cell Biol. 69: 463–474.

Motley AM, Hettema EH, Ketting R, Plasterk R, Tabak, HF (2000). *Caenorhabditis elegans* has a single pathway to target matrix proteins to peroxisomes. EMBO Rep. 1: 40–46.

Mukai S, Ghaedi K, Fujiki Y (2002) Intracellular localization, function, and dysfunction of the peroxisome-targeting signal type 2 receptor, Pex7p, in mammalian cells. J. Biol. Chem. 277: 9548-9561

Nadler-Holly M, Breker M, Gruber R, Azia A, Gymrek M, Eisenstein M, Willison KR, Schuldiner M, Horovitz A (2012) Interactions of subunit CCT3 in the yeast chaperonin CCT/TRiC with Q/N-rich proteins revealed by

high-throughput microscopy analysis. Proc. Natl. Acad. Sci. U S A 109: 18833-18838

Nair DM, Purdue PE, Lazarow PB (2004) Pex7p translocates in and out of peroxisomes in *Saccharomyces cerevisiae*. J. Cell Biol. 167: 599-604

Nakagawa T, Suzuki T, Murata S, Nakamura S, Hino T, Maeo K, Tabata R, Kawai T, Tanaka K, Niwa Y, Watanabe Y, Nakamura K, Kimura T, Ishiguro S (2007) Improved Gateway binary vectors: high-performance vectors for creation of fusion constructs in transgenic analysis of plants. Biosci. Biotechnol. Biochem. 71: 2095-2100

Nito K, Hayashi M, Nishimura M (2002) Direct interaction and determination of binding domains among peroxisomal import factors in *Arabidopsis thaliana*. Plant Cell Physiol. 43: 355–366.

Nito K, Kamigaki A, Kondo M, Hayashi M, Nishimura M (2007) Functional classification of Arabidopsis peroxisome biogenesis factors proposed from analyses of knockdown mutants. Plant Cell Physiol. 48: 763-774

Okumoto K, Abe I, Fujiki Y (2000) Molecular anatomy of the peroxin Pex12p: ring finger domain is essential for Pex12p function and interacts with the peroxisome-targeting signal type 1-receptor Pex5p and a ring peroxin, Pex10p. J. Biol. Chem. 275: 25700-25710

Otera H, Harano T, Honsho M, Ghaedi K, Mukai S, Tanaka A, Kawai A, Shimizu N, Fujiki Y (2000) The mammalian peroxin Pex5pL, the longer isoform of the mobile peroxisome targeting signal (PTS) type 1 transporter, translocates the Pex7p.PTS2 protein complex into peroxisomes via its initial docking site, Pex14p. J. Biol. Chem. 275: 21703-21714

Platta HW, El Magraoui F, Baumer BE, Schlee D, Girzalsky W, Erdmann R (2009) Pex2 and Pex12 Function as Protein-Ubiquitin Ligases in Peroxisomal Protein Import. Mol. Cell Biol. 29: 5505-5516

Platta HW, El Magraoui F, Schlee D, Grunau S, Girzalsky W, Erdmann R (2007) Ubiquitination of the peroxisomal import receptor Pex5p is required for its recycling. J. Cell Biol. 177: 197-204

Purdue PE, Lazarow PB (2001) Pex18p is constitutively degraded during peroxisome biogenesis. J. Biol. Chem. 276: 47684-47689

Reumann S, Babujee L, Ma C, Wienkoop S, Siemsen T, Antonicelli GE, Rasche N, Luder F, Weckwerth W, Jahn O (2007) Proteome analysis of Arabidopsis leaf peroxisomes reveals novel targeting peptides, metabolic pathways, and defense mechanisms. Plant Cell 19: 3170-3193

Reumann S, Quan S, Aung K, Yang P, Manandhar-Shrestha K, Holbrook D, Linka N, Switzenberg R, Wilkerson CG, Weber APM, Olsen LJ, Hu J (2009) In-Depth Proteome Analysis of Arabidopsis Leaf Peroxisomes Combined with in Vivo Subcellular Targeting Verification Indicates Novel Metabolic and Regulatory Functions of Peroxisomes. Plant Physiol. 150: 125-143

Rutherford S, Moore I (2002) The Arabidopsis Rab GTPase family: another enigma variation. Curr. Opin. Plant Biol. 5: 518-528

Schuhmann H, Huesgen PF, Gietl C, Adamska I (2008) The DEG15 serine protease cleaves peroxisomal targeting signal 2-containing proteins in Arabidopsis. Plant Physiol. 148: 1847-1856

Schumann U, Prestele J, O'Geen H, Brueggeman R, Wanner G, Gietl C (2007) Requirement of the C3HC4 zinc RING finger of the Arabidopsis PEX10 for photorespiration and leaf peroxisome contact with chloroplasts. Proc. Natl. Acad. Sci. U S A 104: 1069-1074

Sichting M, Schell-Steven A, Prokisch H, Erdmann R, Rottensteiner H (2003) Pex7p and Pex20p of *Neurospora crassa* function together in PTS2-dependent protein import into peroxisomes. Mol. Biol. Cell 14: 810-821

Singh T, Hayashi M, Mano S, Arai Y, Goto S, Nishimura M (2009) Molecular components required for the targeting of PEX7 to peroxisomes in *Arabidopsis thaliana*. Plant J. 60: 488-498

Tabak HF, Murk JL, Braakman I, Geuze HJ (2003) Peroxisomes start their life in the endoplasmic reticulum. Traffic 4: 512-518

Tamura K, Fukao Y, Iwamoto M, Haraguchi T, Hara-Nishimura I (2010) Identification and characterization of nuclear pore complex components in Arabidopsis thaliana. Plant Cell 22, 4084-4097

Titorenko VI, Rachubinski RA (1998) Mutants of the yeast *Yarrowia lipolytica* defective in protein exit from the endoplasmic reticulum are also defective in peroxisome biogenesis. Mol. Cell Biol. 18(5):2789-2803

Tolbert NE (1982) Leaf peroxisomes. Ann. N. Y. Acad. Sci. 386: 254–268.

Valpuesta JM, Benito JM, Puertas PG, Carrascosa JL, Willison KR (2002) Structure and function of a protein folding mahine: the eukaryotic cytosolic chaperonin CCT. FEBS J. 529, 11–16

van der Zand A, Gent J, Braakman I, Tabak HF (2012) Biochemically distinct vesicles from the endoplasmic reticulum fuse to form peroxisomes. Cell 149: 397-409

Verheyden K, Fransen M, Van Veldhoven PP, Mannaerts GP (1992) Presence of small GTP-binding proteins in the peroxisomal membrane. Biochim. Biophys. Acta. 1109: 48-54

Woodward AW, Bartel B (2005) The Arabidopsis peroxisomal targeting signal type 2 receptor PEX7 is necessary for peroxisome function and dependent on PEX5. Mol. Biol. Cell 16: 573-583

Woollard AA, Moore I (2008) The functions of Rab GTPases in plant membrane traffic. Curr. Opin. Plant Biol. 11: 610-619

Yaffe MB, Farr GW, Miklos D, Horwich AL, Sternlicht ML, Sternlicht H (1992) Tcp1 Complex Is a Molecular Chaperone in Tubulin Biogenesis. Nature 358: 245-248

Yahraus T, Braverman N, Dodt G, Kalish JE, Morrell JC, Moser HW, Valle D, Gouldl SJ (1996) The peroxisome biogenesis disorder group 4 gene, PXAAA1,encodeses cytoplasmic ATPase required for stability of the PTS1 receptor. EMBO J. 15(12): 2914-2923

Yi C, Li S, Wang J, Wei N, Deng XW (2006) Affinity purification reveals the association of WD40 protein constitutive photomorphogenic 1 with the

hetero-oligomeric TCP-1 chaperonin complex in mammalian cells. Int. J. Biochem. Cell Biol. 38: 1076-1083

Yonekawa S, Furuno A, Baba T, Fujiki Y, Ogasawara Y, Yamamoto A, Tagaya M, Tani K (2011) Sec16B is involved in the endoplasmic reticulum export of the peroxisomal membrane biogenesis factor peroxin 16 (Pex16) in mammalian cells. Proc. Natl. Acad. Sci. U S A 108: 12746-12751

Yu JH, Goh J, Jeon J, Kim KS, Park J, Park SY, Lee YH (2011) The PEX7-mediated peroxisomal import system is required for fungal development and pathogenicity in magnaporthe oryzae. PLoS One 6: e28220

Zhang JW, Lazarow PB (1995) PEB1 (PAS7) in *Saccharomyces cerevisiae* encodes a hydrophilic, intro-peroxisomal peotein that is a member of the WD repeat family and is essential for the import of thiolase into peroxisomes. J. Cell Biol. 129(1): 65-80

Zhang X, Hu J (2009) Two small protein families, DYNAMIN-RELATED PROTEIN3 and FISSION1, are required for peroxisome fission in Arabidopsis. Plant J. 57: 146-159

Zhang X, Hu J (2010) The Arabidopsis chloroplast division protein DYNAMIN-RELATED PROTEIN5B also mediates peroxisome division. Plant Cell 22: 431-442

Zheng H, Camacho L, Wee E, Batoko H, Legen J, Leaver CJ, Malho R, Hussey PJ, Moore I (2005) A Rab-E GTPase mutant acts downstream of the Rab-D subclass in biosynthetic membrane traffic to the plasma membrane in tobacco leaf epidermis. Plant Cell 17: 2020-2036

Zolman BK, Bartel B (2004) An Arabidopsis indole-3-butyric acid-response mutant defective in PEROXIN6, an apparent ATPase implicated in peroxisomal function. Proc. Natl. Acad. Sci. U S A 101: 1786-1791

Zolman BK, Yoder A, Bartel B (2000) Genetic analysis of indole-3-butyric acid responses in *Arabidopsis thaliana* reveals four mutant classes. Genetics 156: 1323-1337

Tables

Table 1.1. Proteins coimmunoprecipitated with GFP-PEX7 in the both DDM and digitonin experiments.

AGI code	Annotation	Score in DDM	Score in Digitonin
AT1G29260.1	PEX7 (PEROXIN 7)	1764	1544
AT5G20890.1	T-complex protein 1, β subunit	573	278
AT3G20050.1	T-complex protein 1, α subunit	532	581
AT3G03960.1	T-complex protein 1, θ subunit	501	413
AT1G55490.1	CPN60B (CHAPERONIN 60 β)	455	67
AT3G02530.1	T-complex protein 1, ζ subunit	420	243
AT5G16070.1	T-complex protein 1, ζ subunit	389	236
AT1G24510.1	T-complex protein 1, ε subunit	372	195
AT5G42080.1	DRP1A (Arabidopsis dynami-related protein 1A)	356	110
AT3G11830.1	T-complex protein 1, η subunit	318	288
AT3G18190.1	T-complex protein 1, δ subunit	296	209
AT5G26360.1	T-complex protein 1, γ subunit	190	200
AT5G56290.1	PEX5 (PEROXIN 5)	172	207
AT3G46060.1	AtRABE1c (Arabidopsis Rab GTPase homolog E1c)	78	55
AT4G18430.1	AtRABA1e (Arabidopsis Rab GTPase homolog A1e)	56	73

Table 1.2. Proteins coimmunoprecipitated with GFP-PEX16 in the both DDM and digitonin experiments.

AGI code	Annotation	Score in Digitonin	Score in DDM
AT2G45690.1	PEX16 (PEROXIN 16)	10029	5356
AT5G10890.1	Myosin heavy chain-related (PEX16 binding protein 1/PBP1)	110	60
AT5G06350.1	ARM repeat superfamily protein (PEX16 binding protein 2/PBP2)	82	54

Table 1.3. Proteins coimmunoprecipitated with GFP-PTS1 in the both DDM and digitonin experiments.

AGI code	Annotation	Score in Digitonin	Score in DDM
AT5G67360.1	ARA12 (subtilase)	2182	2376

Table 1.4. Proteins coimmunoprecipitated with GFP-PEX7 and GFP-PEX16 in the both DDM and digitonin experiments.

		GFP-PEX7		GFP-PEX16	
AGI code	**Annotation**	**Score in DDM**	**Score in Digitonin**	**Score in DDM**	**Score in Digitonin**
AT4G28520.1	CRU3 (CRUCIFERIN 3), nutrient reservoir	716	1115	184	1054
AT5G44120.3	CRA1 (CRUCIFERINA), nutrient reservoir	306	677	225	404
AT2G38750.1	ANNAT4 (ANNEXIN ARABIDOPSIS 4), calcium ion binding / calcium-dependent phospholipid binding	157	124	137	93
AT4G35090.1	CAT2 (CATALASE 2), catalase	123	178	139	150
AT1G20630.1	CAT1 (CATALASE 1), catalase	90	176	72	127
AT3G58570.1	DEAD box RNA helicase, putative	64	206	61	94

Table 1.5. Proteins coimmunoprecipitated with GFP-PTS1, GFP-PEX7 and GFP-PEX16 in the both DDM and digitonin experiments.

		GFP-PTS1		GFP-PEX7		GFP-PEX16	
AGI code	**Annotation**	**Score in DDM**	**Score in Digitonin**	**Score in DDM**	**Score in Digitonin**	**Score in DDM**	**Score in Digitonin**
AT3G27660.1	OLEO4 (OLEOSIN4)	492	303	1687	1067	1406	804
AT3G01570.1	glycine-rich protein / oleosin	425	301	1073	777	912	484
AT5G40420.1	OLEO2 (OLEOSIN 2)	256	231	1185	955	1033	516
AT5G02500.1	HSC70-1 (heat shock cognate	154	679	166	673	104	350
AT4G21280.1	PSBQ/PSBQ-1/PSBQA, calcium	132	354	99	183	182	227
AT3G15356.1	Legume lectin family protein	120	195	128	97	268	255
AT4G25140.1	OLEO1 (OLEOSIN1)	99	157	847	562	530	414
AT3G25220.1	FKBP15-1 (FK506-binding protein 15 kD-1), FK506 binding / peptidyl-prolyl cis-trans	92	105	90	67	63	128
AT1G07920.1	Elongation factor 1-alpha / EF-1-	75	112	350	735	330	374
AT3G03305.1	Calcineurin-like phosphoesterase family protein	68	94	61	77	75	67

Table 1.6. PTS1 and PTS2 proteins identified with GFP-PEX7 specifically.

AGI code	Annotation	Score in Digitonin	Score in DDM	type of PTS
AT1G71695.1	PER12 (PEROXIDASE 12)	52	34	1
AT5G27600.1	LACS7 (LONG-CHAIN ACYL-COA SYNTHETASE 7)	34	51	1,2
AT5G47040.1	LON2 (LON PROTEASE 2)		530	1
AT3G14415.1	GOX2 (GLYCOLATE OXIDASE 2)		117	1
AT1G54340.1	ICDH (ISOCITRATE DEHYDROGENASE)		64	1
AT2G42490.1	Copper amine oxidase		46	1
AT5G09660.2	PMDH2 (PEROXISOMAL NAD-MALATE DEHYDROGENASE 2)		32	2
AT1G65520.1	Enoyl-CoA hydratase/isomerase family protein		23	1

Figures

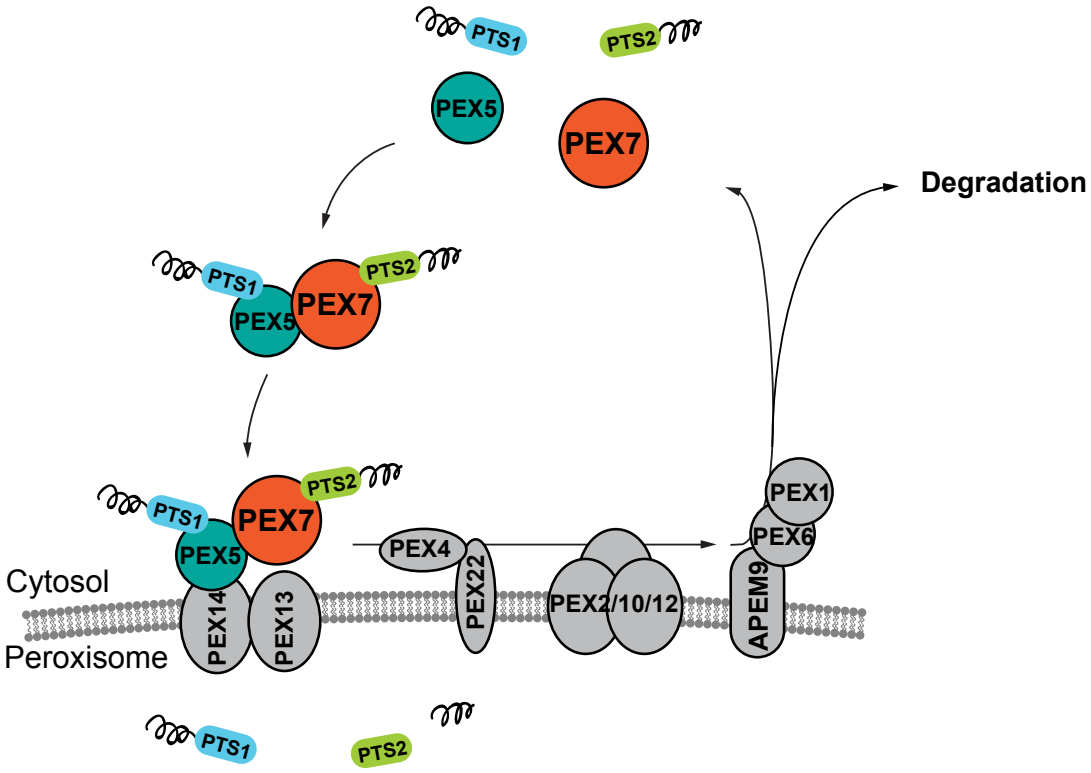

Figure 1. Model for the peroxisomal protein transport mediated by two receptors, PEX5 and PEX7.
PTS1- and PTS2-containing proteins are captured by their receptors, PEX5 and PEX7, respectively. They form a cytosolic receptor-cargo complex through the interaction between PEX5 and PEX7. This complex is docked on the peroxisomal membranes upon the interaction between PEX5 and PEX14, where the PTS1 and PTS2 cargos are released into peroxisomal matrix. PEX13 and PEX14 forms docking complex. PEX5 and PEX7 complexes are translocated and recycled back to the cytosol or to the degradation pathway by other peroxisomal membrane protein complexes including APEM9, PEX1, PEX2, PEX4, PEX6, PEX10 and PEX12.

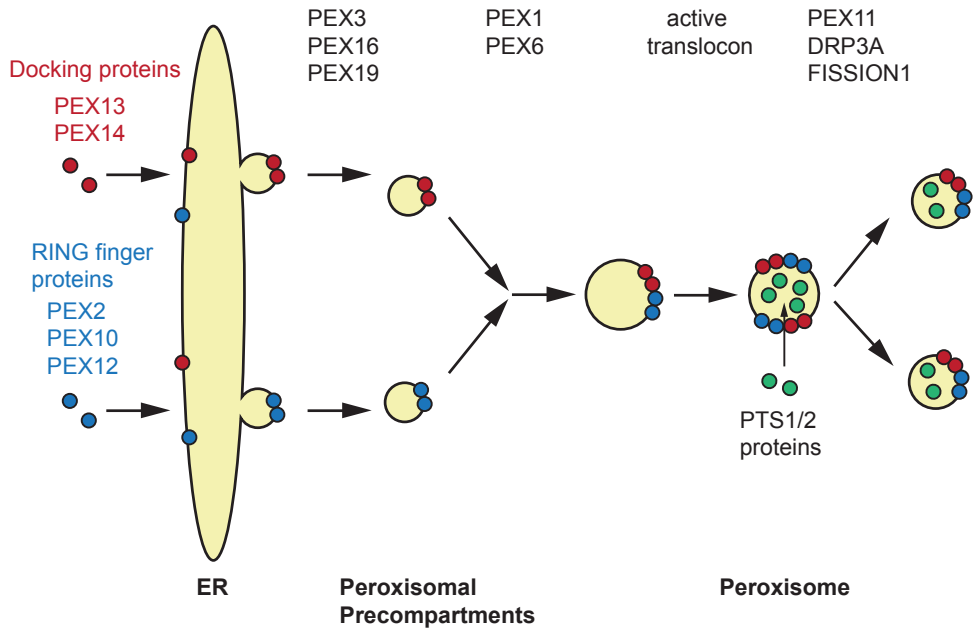

Figure 2. Model for peroxisomal biogenesis mediated through various peroxisomal membrane proteins.
Docking proteins (PEX13, PEX14) and RING finger proteins (PEX2, PEX10, PEX12) insert into ER, where they form two distinct vesicles of peroxisomal precompartments. The vesicles are budded from ER via PEX3, PEX16 and PEX19 and later combine with each other through PEX1 and PEX6. This fusion allows assembly of the full peroxisomal translocon and the start of peroxisomal matrix protein transport from the cytosol. This completes the formation of mature peroxisomes which subsequently undergoes division by PEX11, DRP2A and FISSION1.

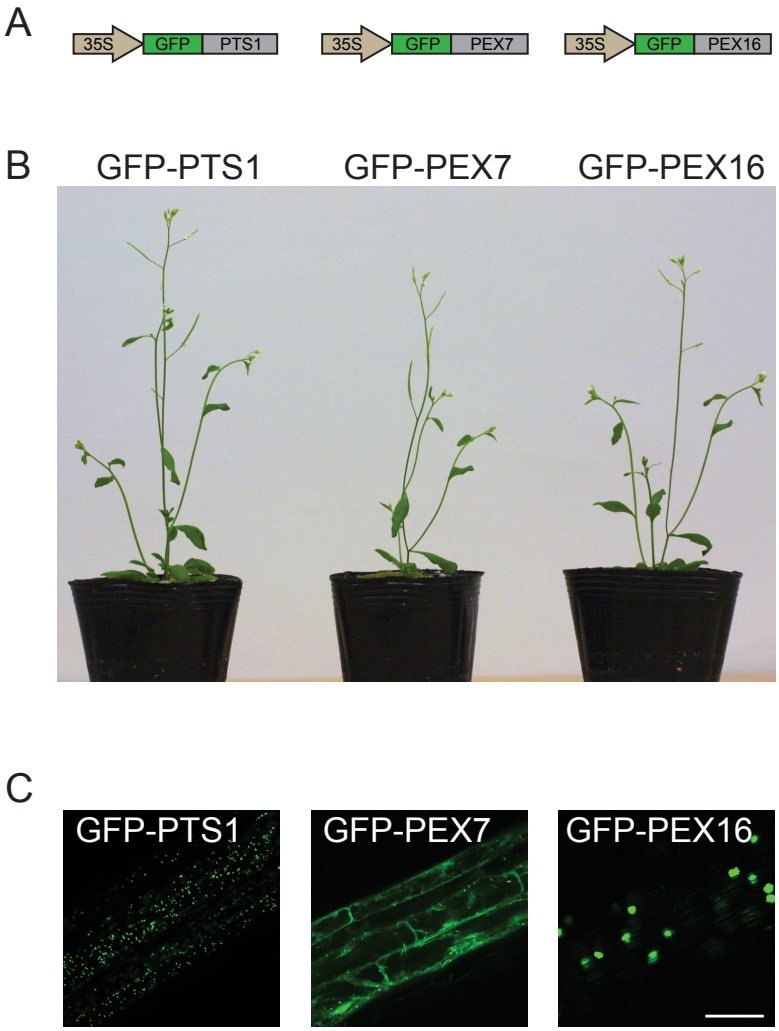

Figure 1.1. Establishment of transgenic plants overexpressing GFP-PTS1, GFP-PEX7 and GFP-PEX16.
(A) Diagram representing the constructs used for the establishment of transgenic plants. Peroxisome targeting signal 1 (PTS1), PEX7 and PEX16 were each fused with green fluorescence protein (GFP) under the control of CaMV 35S promoter. Each chimeric gene was introduced into *Arabidopsis thaliana* to generate stable transgenic plants.
(B) The growth of 4-week-old transgenic plants grown at 22°C with light duration of 16 h light and 8 h dark.
(C) Fluorescence images from the GFP-PTS1, GFP-PEX7 or GFP-PEX16 overexpressing plants. Root tissue was observed under confocal microscopy. Bar = 50 μm.

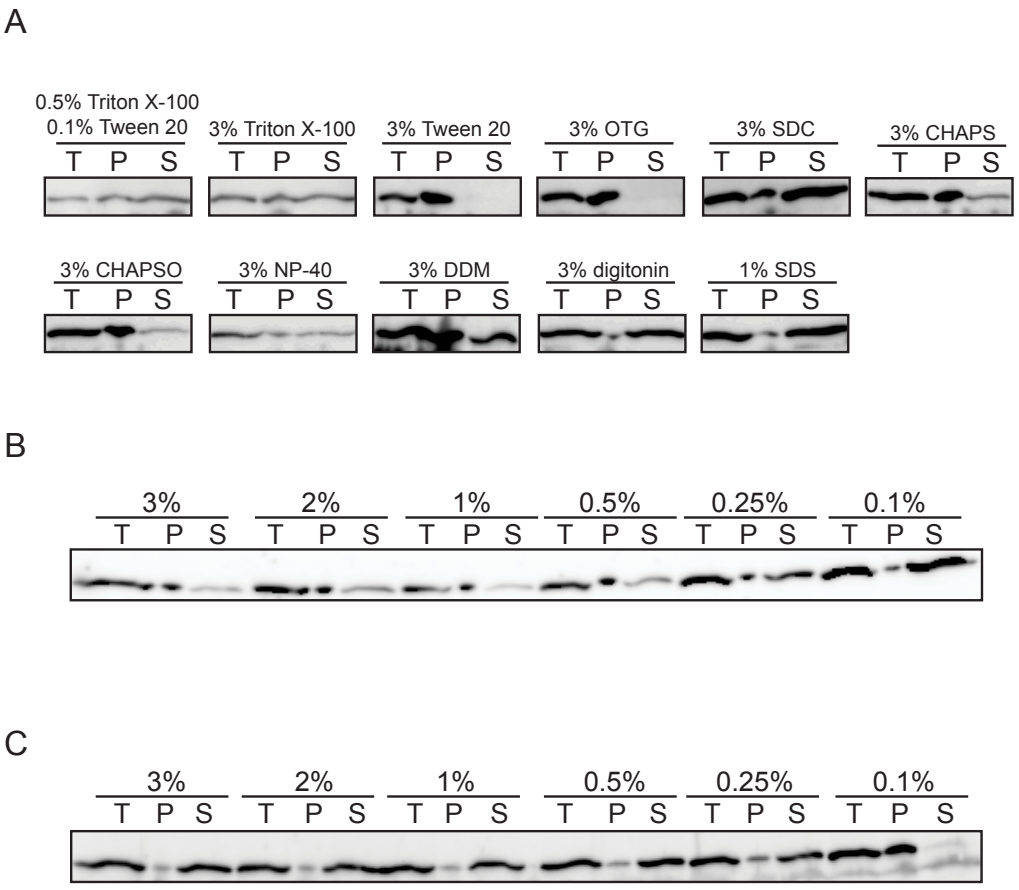

Figure 1.2. Determination of the detergent for efficient solubilization of peroxisomal membrane protein, GFP-PEX16.
(A) GFP-PEX16 transgenic seedlings grown in dark for 7 days were homogenized in the buffer containing various detergents that are indicated on the top of each panel. Their final concentrations are indicated in the left of each detergent. The homogenates (T) were subsequently fractionated into pellet (P) and soluble fraction (S) by centrifugation at 100,000 × g. Equal amount of proteins in each fraction were applied to SDS-PAGE followed by immunoblot with anti-GFP to detect GFP-PEX16. Note that GFP-PEX16 was sufficiently solubilized in n-dodecyl β-D-maltoside (DDM) and digitonin.
(B-C) Various concentrations of DDM (B) and digitonin (C) were used to solubilized GFP-PEX16 using the method described above. Note that GFP-PEX16 was efficiently solubilized in the buffer containing 0.1% DDM and 0.25% digitonin, respectively.

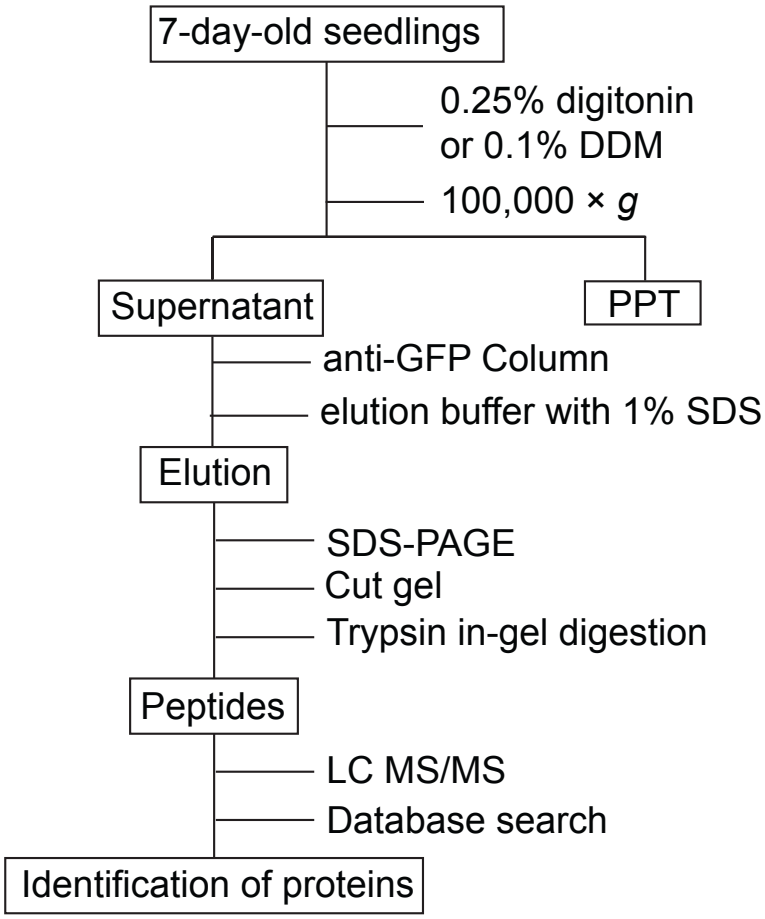

Figure 1.3. Schematic representation showing the procedure for isolation of fusion protein complexes and identification of their protein components.
The seedlings of GFP-PTS1, GFP-PEX7 or GFP-PEX16 grown for 7 days under dark condition were homogenized independently using homogenization buffer containing detergent of digitonin or dodecylmaltoside (DDM). After ultracentrifugation, the supernatant from each transgenic seedlings was immunoprecipitated with anti-GFP antibodies. Each elution fraction was seperated by SDS-PAGE, digested by trypsin and applied to LTQ-Orbitrap mass spectrometry. Protein scores were calculated by Mascot database (Matrix Science).

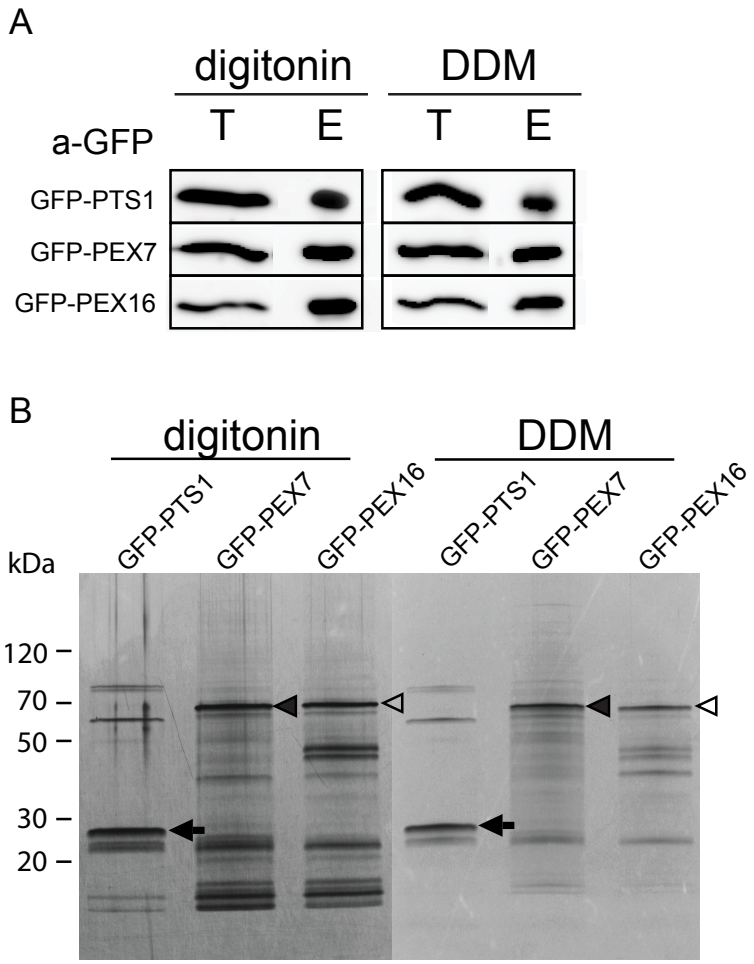

Figure 1.4. The efficiency of protein complex isolation by immunoprecipitation.
(A) Isolation of GFP-fusion proteins from transgenic Arabidopsis plants expressing GFP-PEX7, GFP-PTS1 and GFP-PEX16. Total extracts were prepared from the plants in the presence of either n-dodecyl β-D-maltoside (DDM) or digitonin. The GFP-fusion protein in the extracts was immunoprecipitated with an anti-GFP antibody. The amounts of fusion protein contained in 20 µl of total extract (T) or an equal volume of elution fraction (E) were compared by SDS-polyacrylamide gel electrophoresis followed by immunoblot with an anti-GFP antibody. (B) Proteins that coimmunoprecipitated with the GFP-fusion proteins. Proteins in the elution fraction were subjected to SDS-polyacrylamide gel electrophoresis and visualized by silver staining. The transgenic plant type and the detergent used are indicated above each lane. The positions of the GFP-PEX7, GFP-PTS1, and GFP-PEX16 proteins are indicated by an arrow, closed and open arrowheads, respectively.

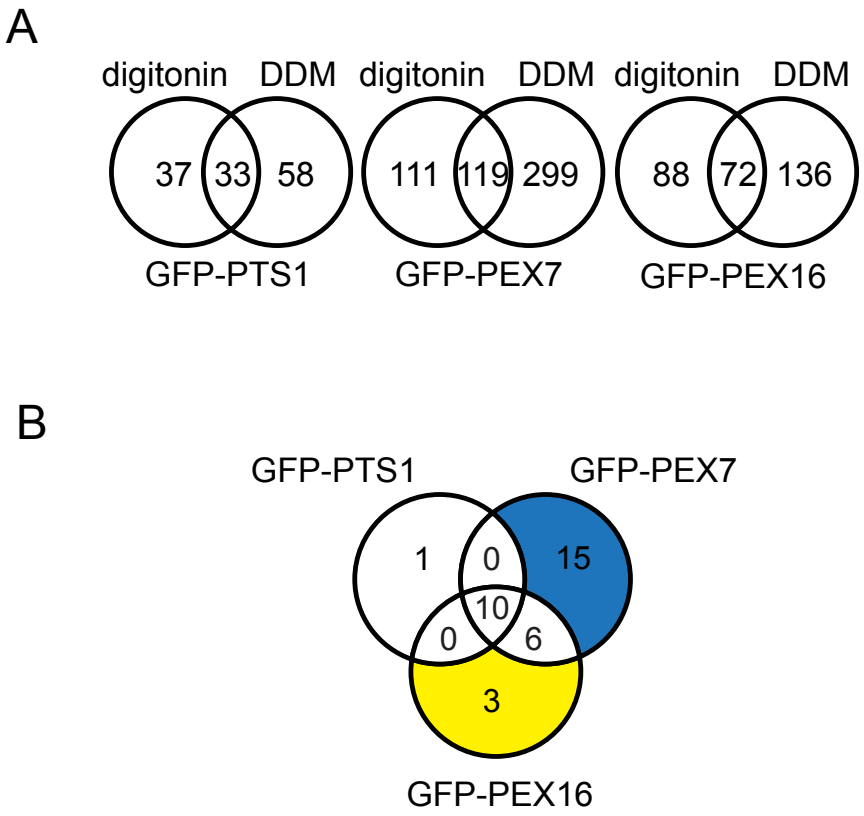

Figure 1.5. Schematic representation for the number of proteins in affinity purified fractions after MS/MS analysis.
Venn diagram representing the number of protein candidates that bind with each GFP-fusion protein. (A) The number in each circle indicates proteins identified in digitonin or DDM treated samples of GFP-PTS1, GFP-PEX7 and GFP-PEX16. Overlapping region shows the number of proteins appearing both in digitonin and DDM experiments. (B) Proteins with protein scores over 50 were selected from the overlapping region in (A) and compared with each other. A total of 1, 15 and 3 proteins were specifically identified in GFP-PTS1, GFP-PEX7 and GFP-PEX16, respectively. Six proteins were identified from GFP-PEX7 and GFP-PEX16 samples in both DDM and digitonin experiments. Ten proteins were from all three samples in both DDM and dititoinin experiments.

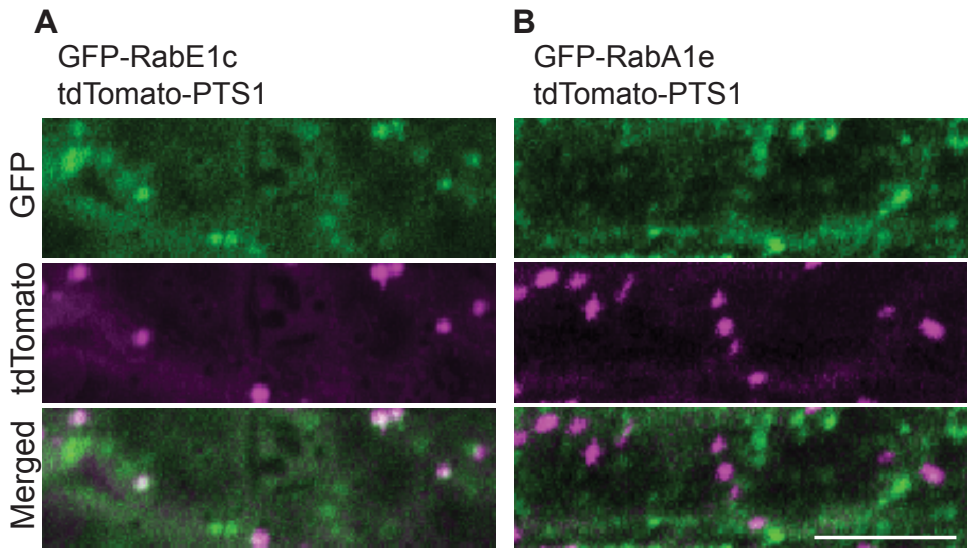

Figure 2.1. Subcellular localization of RabE1c and RabA1e.
Subcellular localization of RabE1c and RabA1e. Either GFP-RabE1c (A) or GFP-RabA1e (B) was introduced together with tdTomato-PTS1 into leek epidermal cells. GFP and tdTomato fluorescence in the cells was visualized by confocal laser scanning microscopy. The green color shown in the top and bottom panels represents fluorescence derived from the GFP-fusion proteins, while the magenta color in the middle and bottom panels represents fluorescence derived from tdTomato-PTS1. White spots in the merged image (A, bottom panel) indicate peroxisomes containing both GFP-RabE1c and tdTomato-PTS1. Scale bar indicates 10 μm.

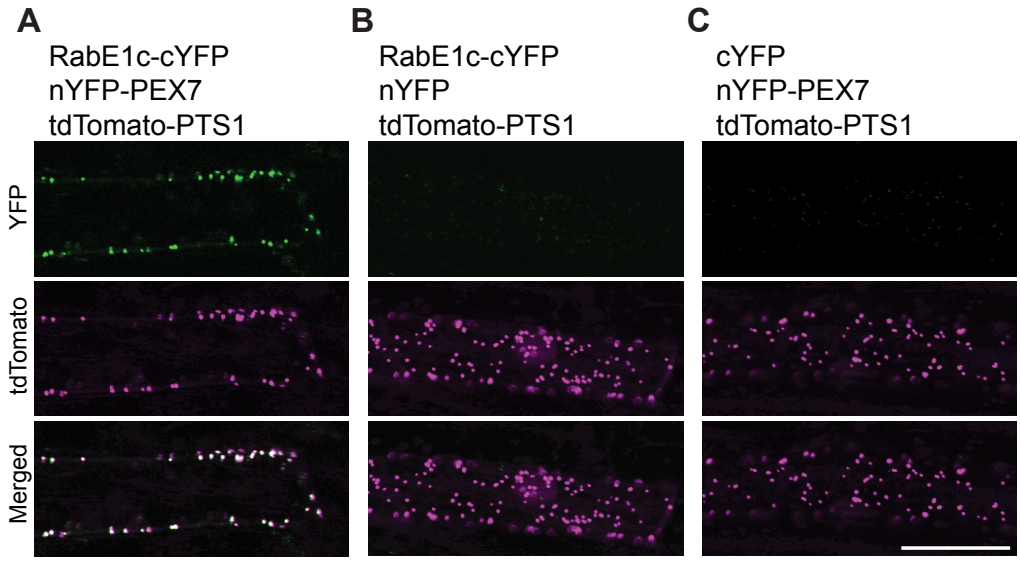

Figure 2.2. Bimolecular fluorescence complementation (BiFC) analysis of the interaction between RabE1c and PEX7.
(A, top panel) RabE1c-cYFP and nYFP-PEX7 were co-expressed in leek epidermal cells. Fluorescence derived from reconstituted YFP was visualized by confocal laser scanning microscopy. As negative controls, fluorescence was also examined in cells co-expressing RabE1c-cYFP/nYFP (B, top panel) and cYFP/nYFP-PEX7 (C, top panel). In all cases, tdTomato-PTS1 was simultaneously expressed as marker for peroxisomes (A-C, middle and bottom panels). White spots in the merged image (A, bottom panel) indicate colocalization of YFP and tdTomato fluorescence. Scale bar indicates 50 μm.

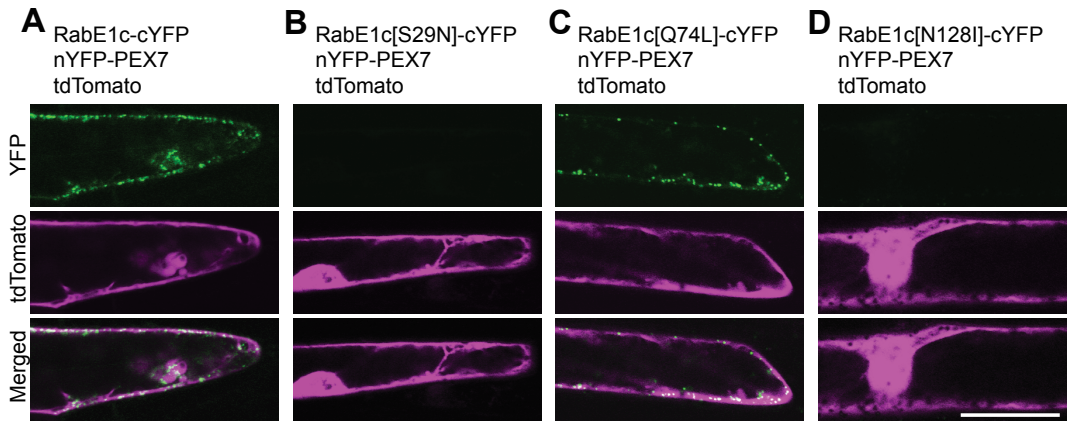

Figure 2.3. Constitutively active form but not dominant negative form of RabE1c interacts with PEX7.

Confocal microscopic images of leek epidermal cells were acquired after coexpression of nYFP-PEX7 with RabE1c-cYFP (A), RabE1c [S29N]-cYFP (B), RabE1c [Q74L]-cYFP (C) and [N128I]-cYFP (D). YFP fluorescence (A and C, top panels) represents reconstituted YFP molecules. Cytosolic tdTomato was simultaneously expressed in all experiments as a marker of transformed cells. Scale bar indicates 50 μm.

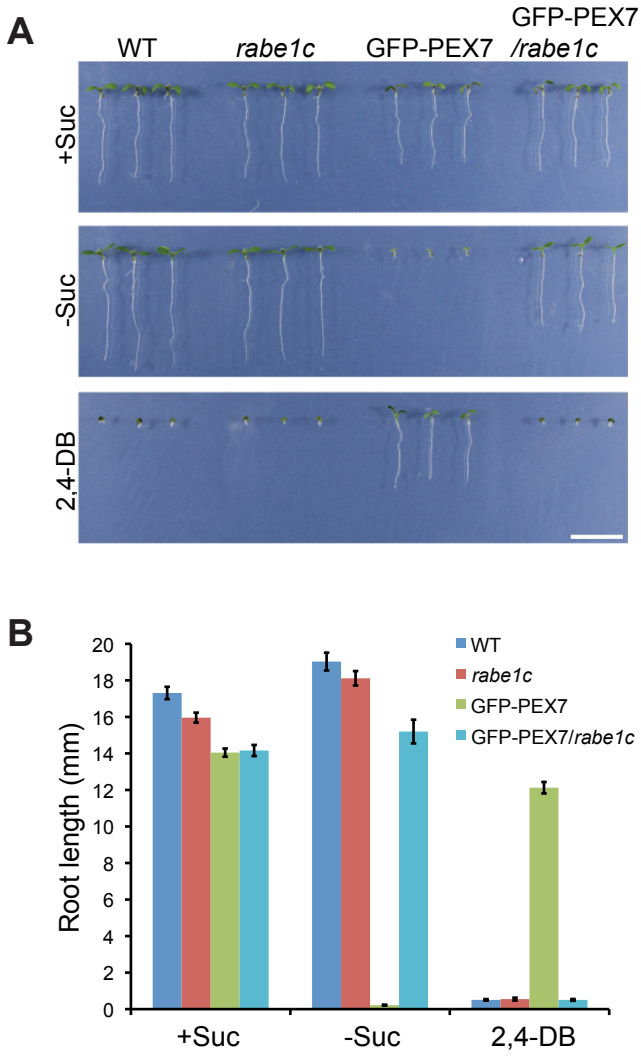

Figure 2.4. Effect of sucrose and 2,4-dichlorophenoxybutyric acid (2,4-DB) on the growth of *rabe1c* mutant.
(A) Wild-type plants, *rabe1c* mutant (*rabe1c*), transgenic plants expressing GFP-PEX7 (GFP-PEX7), and rabe1c mutant crossed with transgenic plants expressing GFP-PEX7 (GFP-PEX7/*rabe1c*) were grown in the presence (+Suc) or absence (-Suc) of sucrose for 6 days under continuous illumination. These plants were also grown in the presence of 0.5 µg/ml 2,4-DB (2,4-DB). Scale bar indicates 1 cm. B. Root lengths of the seedlings shown in (A). Data represents the means ± SD (n=12) in mm.

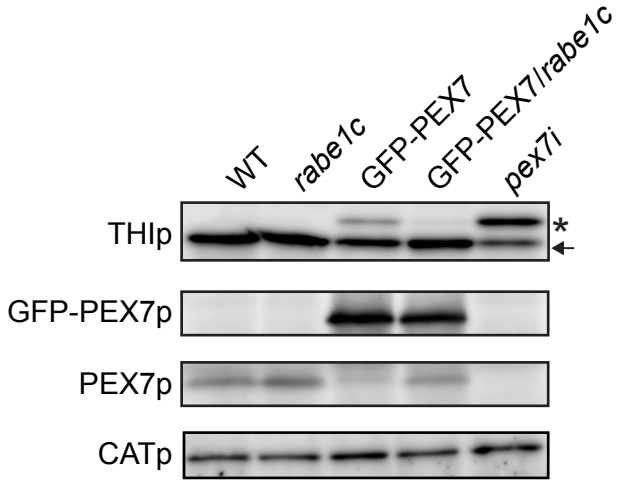

Figure 2.5. PTS2 protein transport and the amount of endogenous PEX7 in mutant seedlings.
Equal amounts of homogenate (50 μg for GFP-PEX7p and PEX7p, 10 μg for CATp) from dark-grown wild-type, *rabe1c*, GFP-PEX7, GFP-PEX7/*rabe1c*, and *pex7i* seedlings were separated by SDS-polyacrylamide gel electrophoresis followed by immunoblot analysis to detect 3-ketoacly-CoA thiolase (THIp), GFP-PEX7 (GFP-PEX7p), endogenous PEX7 (PEX7p) and catalase (CATp). The protein level of catalase, which was used as a loading control, was the same in each sample. An asterisk and an arrow indicate the precursor and mature forms of thiolase, respectively.

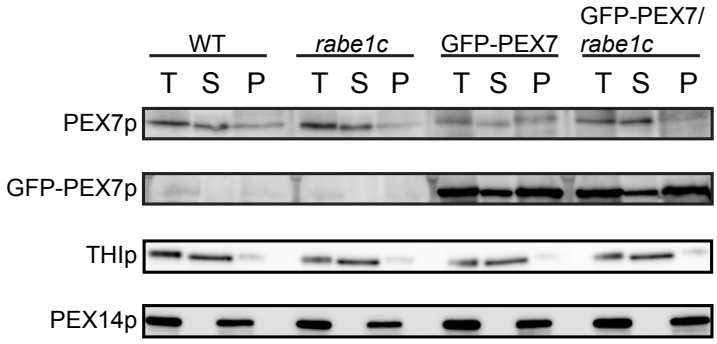

Figure 2.6. Endogenous cytosolic PEX7 is degraded in GFP-PEX7 and restored in GFP-PEX7/*rabe1c* seedlings.

Five-day-old dark-grown wild-type, *rabe1c*, GFP-PEX7 and GFP-PEX7/*rabe1c* seedlings were homogenized in high-salt buffer containing 500 mM NaCl. Total extract (T) was centrifuged at 100,000 × g to separate the supernatant (S) and membrane (P) fractions. Equal amounts of homogenate (50 µg for GFP-PEX7p and PEX7p, 10 µg for THIp and PEX14p) were separated by SDS-polyacrylamide gel electrophoresis followed by immunoblot analysis to detect 3-ketoacly-CoA thiolase (THIp), GFP-PEX7 (GFP-PEX7p), endogenous PEX7 (PEX7p) and PEX14p. Thiolase and PEX14 were used as markers of peroxisomal matrix and membrane proteins, respectively.

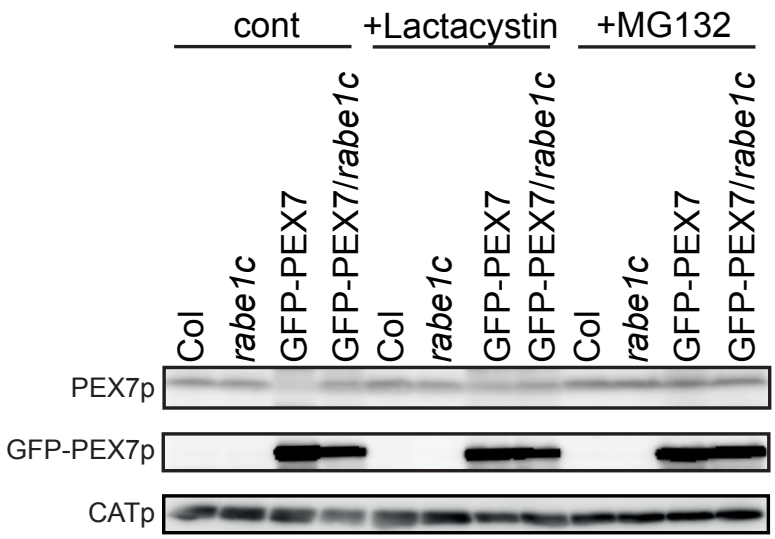

Figure 2.7. The effect of 26S proteasome inhibitor on the amount of endogenous PEX7.

Four-day-old dark-grown wild-type, *rabe1c*, GFP-PEX7 and GFP-PEX7/*rabe1c* seedlings were transferred to liquid MS medium containing 50 μM MG132 or 5 μM lactacystin and incubated for 3 h in the dark. Proteins were then extracted from whole seedlings. Equal amounts of total protein (50 μg) were separated by SDS-polyacrylamide gel electrophoresis followed by immunoblot analyses to detect PEX7 and GFP-PEX7. Catalase (CATp) was used as a loading control.

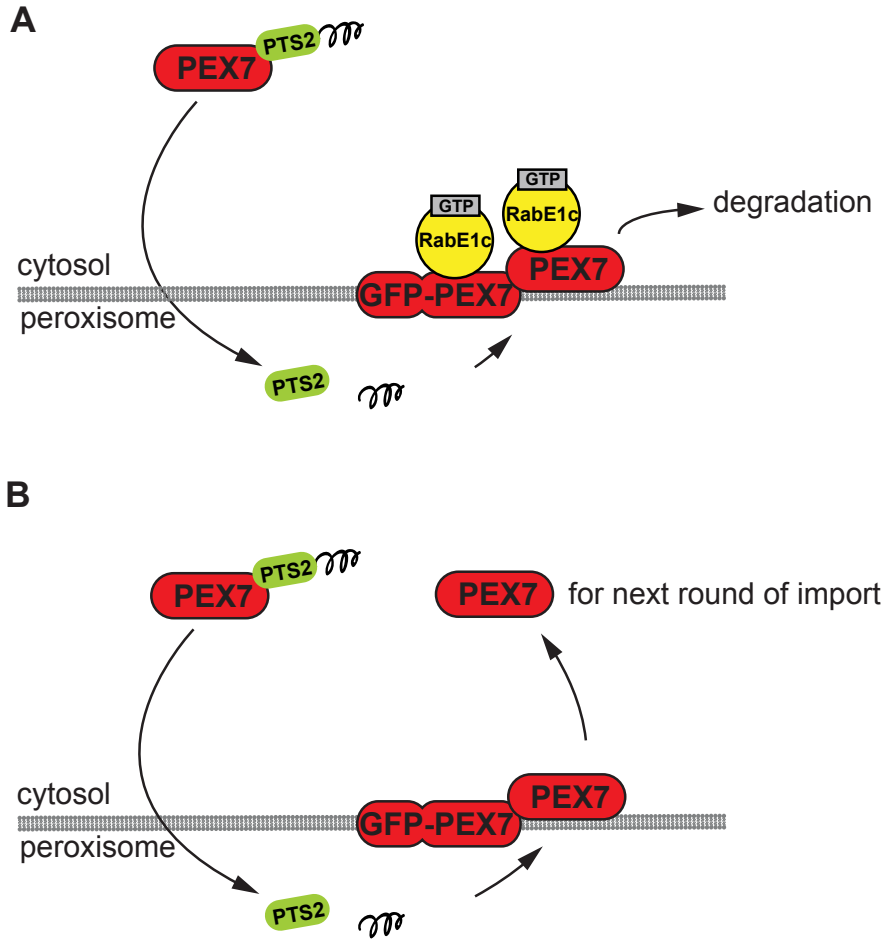

Figure 2.8. Model for the role of RabE1c during export of PEX7 from the peroxisome membrane.
(A) In GFP-PEX7 plants, after the PEX7 receptor-cargo (PTS2-containing protein) complex is imported into the peroxisomes, PEX7 is stacked on the peroxisomal membrane together with GFP-PEX7. The GTP-bound form of RabE1c on the peroxisomal membrane then recruits stacked PEX7 to the 26S proteasome for degradation. RabE1c also binds to GFP-PEX7, but cannot recruit it to the 26S proteasome for degradation. (B) In GFP-PEX7/*rabe1c* plants, the degradation of PEX7 is inhibited, and PEX7 is dislocated into the cytosol for the next round of cargo import. GFP-PEX7 cannot be released into to the cytosol and remains on the peroxisomal membrane.

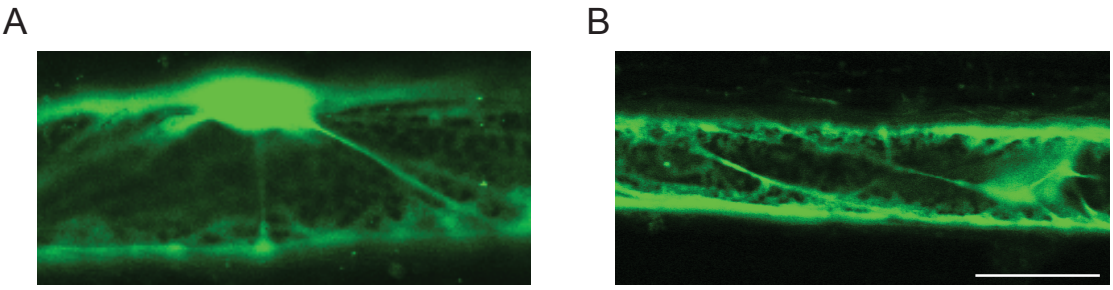

Figure 3.1. Sucellular localization of PBP1 protein in leek epidermal cells.
PBP1 was fused with GFP at either N-terminus (GFP-PBP1) (A) or C-terminus (PBP1-GFP) (B) and transiently expressed in leak epidermal cells. Scale bar indicates 50 μm.

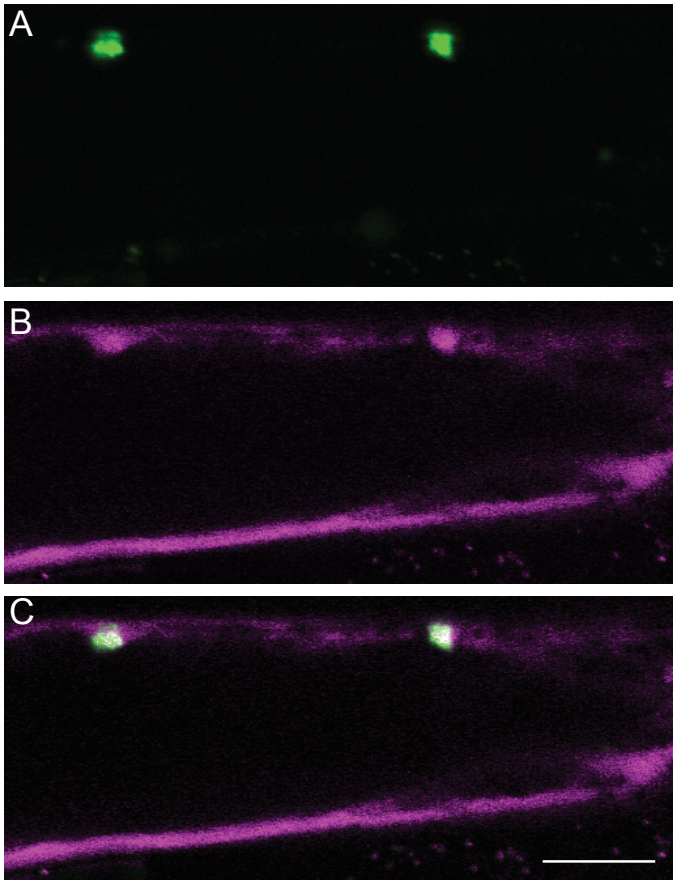

Figure 3.2. Colocalization of PBP1 and PEX16 *in vivo*.
Transient expression of GFP-PEX16 (A) and tdTomato-PBP1 (B) in leek epidermal cells. Green color in (A) indicates GFP-PEX16 in the aggregated peroxisomes and red color in (B) indicates tdTomato-PBP1. The images of (A) and (B) were merged to create the composite image in (C). Bar indicates 20 μm.

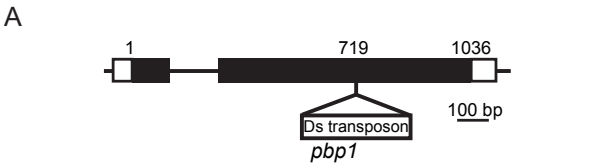

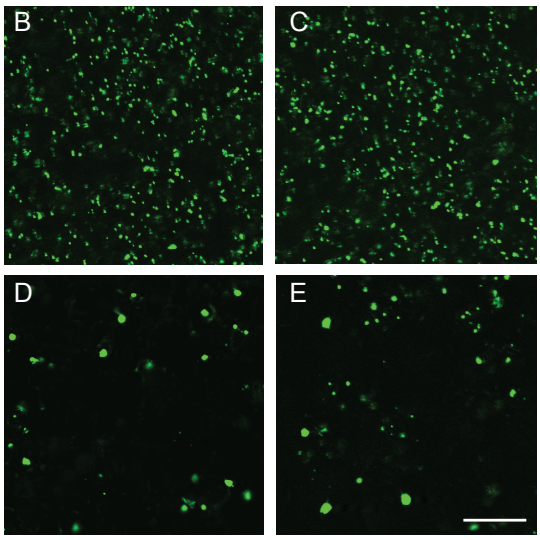

F

```
     PBP1    1 MAEPRVRDSDTVRIRTSSEDDHHR---VGQFSDSPPPTIP  37
AT4G31805    1 MEGSRRRRGDGCTIVQCYTPRRFVGRWLSGLRSSKGKRDA  40
               *   * *  *   *  .    .     .     *

     PBP1   38 SELQ----RREFLFSIGMSCYLIHLIATGRQEIHKIVELR  73
At4g31805   41 GEEQEDDTRRYQLAPIRCSTSLNQLVMQDNKQNCRLNKSK  80
                * *    **  *  *  *. * .*.    ..  ..   .

     PBP1   74 NDLDKFLECRNEE----------------LRQKQQEFVE  96
At4g31805   81 EPETNTFESQSRESPLEVGIGSFLLYLVVASKTELDKMTN 120
                   *..  *                  .

     PBP1   97 LRNDIHKFLEFHNNELRRK--QLEKTETSAYSATSDVVDG 134
At4g31805  121 LRMQMEMFLLNAKEQLQKKDTPMSSNEASGFQFSPQEFSN 160
               **  .  **     .*..*   .  .*.* .  .     .

     PBP1  135 PESSTDHYYSPQIIQTSMSVGGEGSLSHYVYKLENDS--G 172
At4g31805  161 LASSIFQESSSSVLQEEYTEFEVSEPEDYRRGTDCNSKLQ 200
                 **  .  *  ..*   .         *    .  *

     PBP1  173 GEMDQLEAELEAEFELLQIGHNQEVSEDAEGLRLGHVCPG 212
At4g31805  201 AEVGRLPLGEKAEDRQTKHQIQRQCKLKDNEVTKSHIPEM 240
                *. .*     **    .   ...       .   *.

     PBP1  213 LVE-EQQGVCPYELERRLYELMETRQQEEIKELEIALDDA 251
At4g31805  241 VVSDERYGVCPYELDKKLHELLETRQQEELVKLETALNRV 280
               .*  *. *******...* **.*******.  ** **

     PBP1  252 KQRLHLKETEASWWKDTAYIVSERIPEPSR---------- 281
At4g31805  281 ERRLQEKETEVSWWKDAARLLAQRVPESSRSGLEWCNPDS 320
                .**. **** *****.* ....*.** **

     PBP1  282 ITHSSRTHPYPLSR---------- 295
At4g31805  321 STCSERSVPRSYEACSIHRTSFSR 344
                * * *. *
```

Figure 3.3. The effect of PBP1 mutation on peroxisomal morphology in GFP-PTS1 plants and positioning in GFP-PEX16 plants.
(A) Schematic structure of PBP1. Exons are indicated by black boxes. The numbers on the top indicate the position of nucleotide in CDS. Ds transposon is inserted at the second exon of 719bp downstream of start codon. Scale bar = 100 bp.
(B-E) Cotyledonary cells of GFP-PTS1 (B), GFP-PTS1/*pbp1* (C), GFP-PEX16 (D) and GFP-PEX16/*pbp1* (E) plants. Scale bar indicates 50 μm in each figure. (F) Alignment of amino acid sequences of polypeptides encoded by Arabidopsis PBP1 and its homolog At4g31805. The areas in the boxes show the residues appeared in other plant species. Asterisks indicate identical amino acid residues, and dots below the alignment denote similar amino acid replacements.

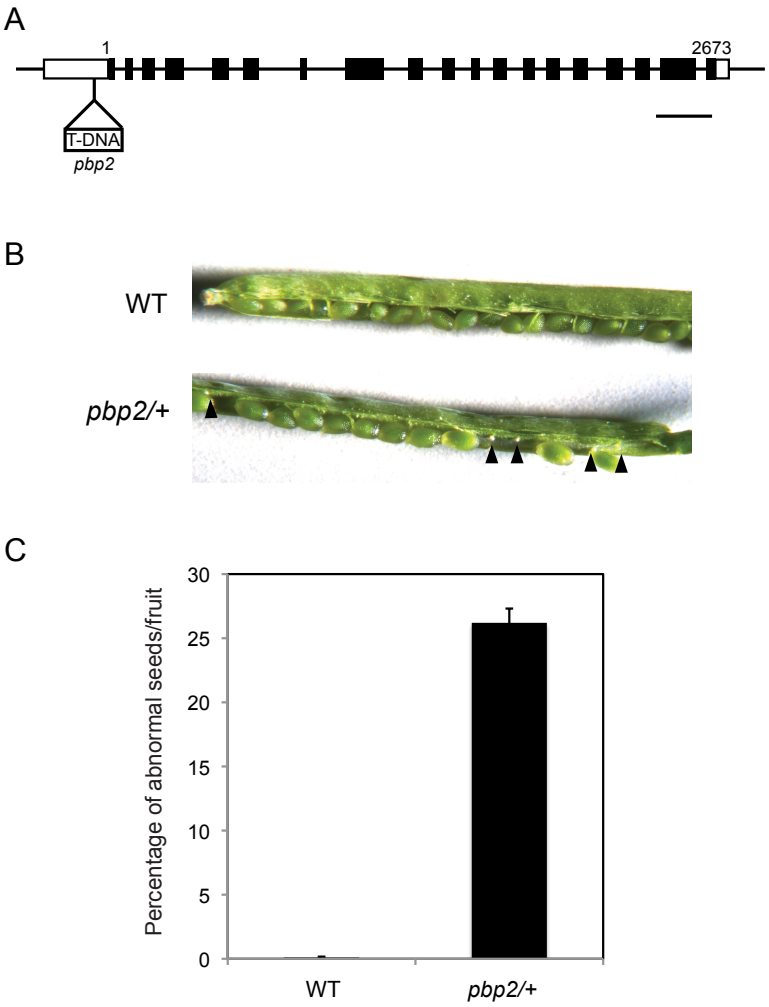

Figure 3.4. Seed establishment in the T-DNA insertion mutant of *pbp2*.
(A) Schematic structure of PBP2. The black and white boxes indicate exons and untranslated regions, respectively. T-DNA was inserted at 148 bp upstream of start codon. Scale bar = 500 bp.
(B and C) pbp2 mutant is lethal. (B) Abnormal seeds in the fruit of the T-DNA insertion line. Images show the seed set in self-fertilized fruits from heterozygote *pbp2* mutant (*pbp2*/+) and wild-type (WT) plant. Black arrowheads indicate the aborted seeds. (C) Proportions of abnormal seeds produced by wild-type (WT) and *pbp2*/+ plant. Data represent means +-SE (n=20).

Acknowledgments

First of all, I wish to express my deepest appreciation to Dr. Mikio Nishimura, Professor of Division of Cell Mechanisms, National Institute for Basic Biology; Department of Basic Biology, School of Life Science, Graduate University for Advanced Studies, for constant supervision and valuable advice and long-term support and encouragement throughout this study.

I am very thankful to Dr. Makoto Hayashi, Dr. Kenji Yamada, Dr. Shoji Mano and all other current and previous members of the Division of Cell Mechanisms, National Institute for Basic Biology, for valuable advice, discussion and kind guidance.

I am also grateful to Dr. Yoichiro Fukao, Associate Professor of Proteomics Groups, Plant Protein Biology, Plant Global Educational Project, The Graduate School of Biological Sciences, Nara Institute of Science and Technology, for conducting the mass spectrometry analysis and providing the proteomics data involved in this project.

Also, I am deeply appreciated to Prof. Nishimura, Mrs. Ueda and all other current and previous members of the Division of Cell Mechanisms, National Institute for Basic Biology, for constant concern and kind support to my foreign life during the study in Japan and the encouragement to get though all the difficulties from the beginning.

Finally, I am grateful to my family for their support and strong belief throughout the work.

January 2013

The Author